

40
38 p.

UCRL-JC-121522
PREPRINTED

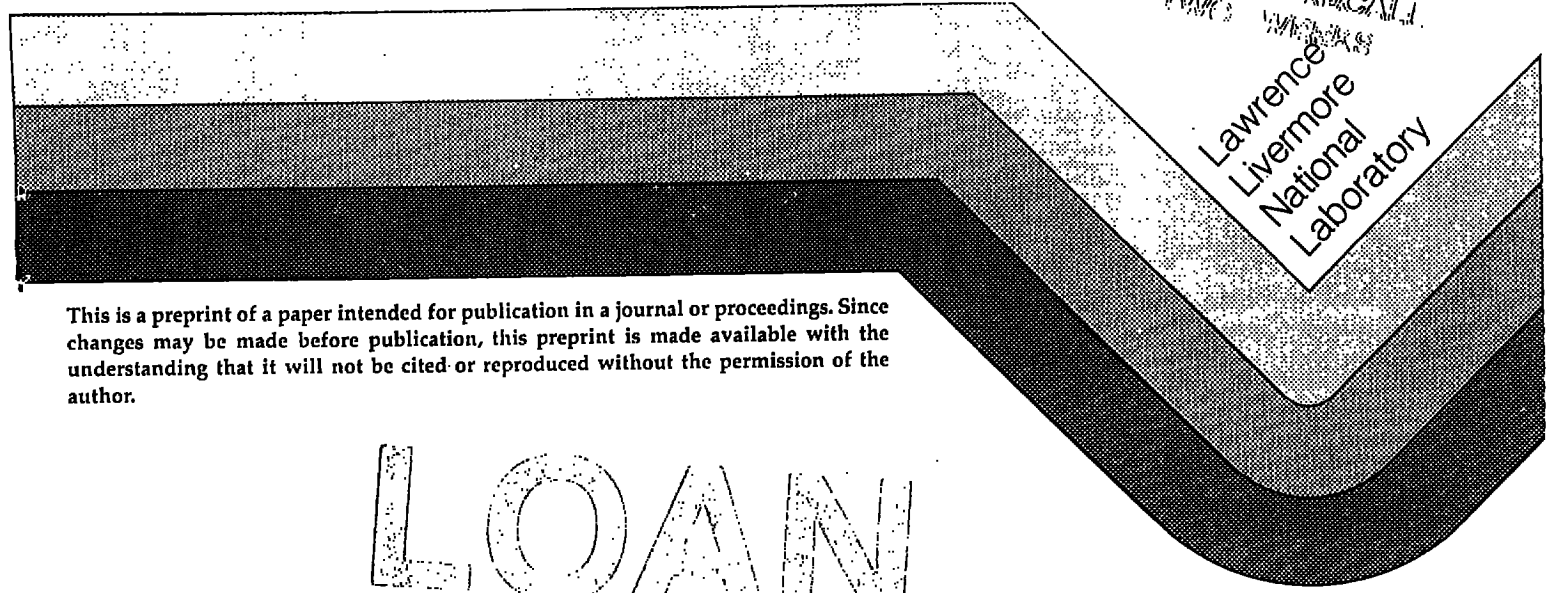
Propagation Characteristics of Lg Across the Tibetan Plateau

6887/1 1/20/25

D.E. McNamara
T.J. Owens
W.R. Walter

Bulletin of the Seismological Society of America

July, 1995



CIRCULATION COPY
SUBJECT TO RECALL
IN TWO WEEKS
Lawrence
Livermore
National
Laboratory

This is a preprint of a paper intended for publication in a journal or proceedings. Since changes may be made before publication, this preprint is made available with the understanding that it will not be cited or reproduced without the permission of the author.

LOAN
COPY

DISCLAIMER

This document was prepared as an account of work sponsored by an agency of the United States Government. Neither the United States Government nor the University of California nor any of their employees, makes any warranty, express or implied, or assumes any legal liability or responsibility for the accuracy, completeness, or usefulness of any information, apparatus, product, or process disclosed, or represents that its use would not infringe privately owned rights. Reference herein to any specific commercial product, process, or service by trade name, trademark, manufacturer, or otherwise, does not necessarily constitute or imply its endorsement, recommendation, or favoring by the United States Government or the University of California. The views and opinions of authors expressed herein do not necessarily state or reflect those of the United States Government or the University of California, and shall not be used for advertising or product endorsement purposes.

This report has been reproduced
directly from the best available copy.

Available to DOE and DOE contractors from the
Office of Scientific and Technical Information
P.O. Box 62, Oak Ridge, TN 37831
Prices available from (615) 576-8401, FTS 626-8401

Available to the public from the
National Technical Information Service
U.S. Department of Commerce
5285 Port Royal Rd.,
Springfield, VA 22161

Propagation Characteristics of L_g Across the Tibetan Plateau

D.E. McNamara†, T.J. Owens†, and W.R. Walter§

† Department of Geological Sciences, University of South Carolina, Columbia, SC

§ Earth Sciences Division, Lawrence Livermore National Laboratory, Livermore, CA

Abstract

The relationship between the propagation characteristics of L_g and lateral heterogeneity within the continental crust has been observed for many years. We present a study of the propagation of L_g within the Tibetan Plateau in two parts. The first is a simple, qualitative analysis of L_g amplitude. The second is a quantitative attempt to estimate the frequency dependence of L_g Q within the Tibetan Plateau. From July, 1991 through June, 1992, 11 broadband digital seismic stations were deployed across the east-central Tibetan Plateau (seven along the Qinghai-Tibet highway from Golmud to Lhasa). During this period, 185 local and regional earthquakes were recorded at distances from 150-2000 km allowing us to analyze over 1200 seismograms for L_g propagation. The propagation of L_g has been observed across most of Asia, however, L_g has not been observed for paths crossing the Tibetan Plateau. We are able to analyze paths that both cross the boundaries and are contained within the Tibetan Plateau. The most significant observation from our dataset is that L_g is generated within the Tibetan Plateau and can propagate efficiently to epicentral distances of at least 600 km. For events from outside of the Tibetan Plateau L_g is absent for paths that cross both the Himalayan and Kunlun ranges confirming that the margins of the plateau effectively block L_g transmission.

We invert L_g amplitudes for paths from 52 events that are confined to the Tibetan Plateau for the quality factor, Q . This yields the frequency dependent Q function:

$$Q(f) = 279f^{0.53} \quad (0.5 \leq f \leq 16\text{Hz}).$$

Similar observations in other areas indicate that frequency dependent apparent Q within the Tibetan Plateau is well below that expected for a typical continental interior. Instead it is similar to an area with active tectonics, such as the Basin and Range Province of North America.

Introduction

Regional differences in the attenuation of seismic waves have been recognized since it was noticed that the felt intensity of earthquakes in the western United States decreases faster with epicentral distance for comparable sized earthquakes in the central and eastern United States (Richter, 1958; Nuttli et al., 1979). With the advent and subsequent abundance of modern instrumentation, amplitude measurements with respect to epicentral distance of regional phases, such as *Lg*, have confirmed that attenuation in the western United States is significantly higher than in the eastern United States (Mitchell and Hwang, 1987; Frankel et al., 1990). In fact, it has been observed throughout the world that *Lg* attenuation is higher for regions with active tectonism than for stable continental interiors (Aki, 1980a).

The *Lg* phase is part of the S-wave train that travels with a group velocity of about 3.5 km/s and is prominent on all three components of motion on regional short period seismograms. In stable continental regions, it is observed at distances as great as 4000 km and has been widely used to estimate earthquake magnitudes and seismic moment for events at regional distances (Nuttli, 1973; Hermann and Kijko, 1983). *Lg* has been successfully modeled as a higher mode surface wave (Ewing et al., 1957; Knopoff et al., 1973) however, the group velocity of *Lg* implies that it propagates as multiply reflected shear waves trapped within the crust (Press and Ewing, 1952, Herrin and Richmond, 1960; Bouchon, 1982). It is commonly observed that lateral heterogeneity plays a significant role in shaping the characteristics of the *Lg* signal (Ruzaikin et al., 1977; Kennett et al., 1985). Consequently, *Lg* carries information about the average crustal shear wave velocity and apparent attenuation along its path and has been shown to be sensitive to varying tectonic environments.

The presence of *Lg* is often used to infer the existence of continental crust because *Lg* does not propagate across oceanic crust. It is thought that *Lg* quickly loses energy in the thin waveguide provided by oceanic crust. Also, *Lg* propagation is affected by variations of the crustal waveguide along its path. For example, Aki (1980a) proposed that scattering of *Lg* energy from fractures within the crust, in tectonically active regions, is a major cause of strong *Lg* attenuation. The disruption of *Lg* propagation can also be caused by the lack of a continuous waveguide. For example, strong attenuation of *Lg* can occur in areas where crustal thickness variations exist between the source and receiver (Gregersen, 1984;

Ruzaikin et al., 1977).

The propagation of Lg has been observed across most of Asia and the Indian Shield, however, Lg has not been observed for paths crossing through the Tibetan Plateau (Ruzaikin et al., 1977; Ni and Barazangi, 1983; Bath, 1954; Pec, 1962; Saha, 1961). This effect has been attributed to either scattering due to a change in the crustal thickness and/or structural discontinuities at the boundaries of the plateau or an unusual velocity structure or high attenuation within the plateau. Previous studies were limited since they had to rely on stations outside of the Tibetan Plateau. They were only able to observe Lg for paths that cross the boundaries of the plateau. Consequently, they were not able to distinguish between the effects that the interior of the plateau versus its boundaries may have had on Lg amplitudes.

In this paper we study the nature of Lg propagation and attenuation in two parts. First, we attempt to qualitatively analyze Lg attenuation and blockage by visually inspecting Lg amplitudes for paths crossing through the Tibetan Plateau and surrounding regions. Second, we quantitatively invert Lg amplitudes, from paths restricted to the Tibetan Plateau, for frequency dependent attenuation. We then compare the resultant Tibetan Plateau Q values to other regions around the world. Frequency dependent Q can be modeled as:

$$Q(f) = Q_0 f^\eta \quad (1)$$

where Q_0 is the quality factor, Q , at 1 Hz and f is the frequency. $Q(f)$ values vary considerably depending on the tectonic style of the region of Lg propagation. For example, Chavez and Priestley (1986) found Lg $Q(f)=214f^{0.54}$ within the tectonically active Basin and Range Province of North America while Atkinson (1989) showed that frequency dependent Q in, tectonically stable, southeastern Canada is as high as $Q(f)=1100f^{0.17}$.

Data used in this study were digitally recorded using 3-component, broadband sensors at 11 sites within the central portion of the Tibetan Plateau (Figure 1, Table 1). At 10 of the stations data was collected in an event triggered mode at 40 samples per second (sps). LHASA operated in a continuously recording mode at 5 sps (Figure 1) (Owens et al., 1993a; Owens et al., 1993b). Instrumentation for this experiment consisted of 10 Streckeisen STS-2 sensors and 1 Guralp CMG-3ESP at the TUNL station (Figure 1). The STS-2 and Guralp are both active feedback seismometers. The STS-2 has flat velocity

response between 1/120 Hz and 50 Hz and the CMG-3ESP has corner frequencies of 1/30 Hz and 30 Hz. (for review see Owens et al., 1993a). Over 1200 seismograms from 185 regional events were examined for the existence of Lg . Of these, 52 events provided paths that travel entirely within the Tibetan Plateau. Event locations are determined from the USGS PDEs and are shown in Figure 1 and listed in Table 2.

Lg propagation within the Tibetan Plateau and surrounding regions

Our qualitative analysis of Lg is similar to the method applied by Ruzaikin et al. (1977) and to the mapping of Sn propagation within the Tibetan Plateau (McNamara et al., 1995; Ni and Barazangi, 1983). The procedure is rudimentary and consists of two parts. First, we merely note if Lg is present, absent or weak on both the tangential and radial component high pass filtered (> 0.5 Hz) event record sections at the time appropriate for a wave traveling at a typical continental Lg velocity (3.2-3.6 km/s). A weak Lg arrival is defined as one with an amplitude less than half that of the Pg wave. Second, to better constrain the spatial distribution of Lg propagation characteristics, we map event/station paths, coded to represent our amplitude observations. We were able to observe Lg within a range of path lengths from several hundred to several thousand kilometers. We focused on events with epicentral distances greater than 150 km for two reasons. First, in many cases with short epicentral distances, it was difficult to determine the presence of Lg because of interference with the higher amplitude S arrivals. Second, by using events with distances greater than 150 km we assure a constant geometrical spreading (Street et al., 1975).

The most significant new observations from our dataset is that Lg propagates within the Tibetan Plateau and that both the northern and southern boundaries of the plateau effectively block Lg propagation. We have observed strong Lg at every station from events with epicenters within the plateau. Previous studies have had few recording stations on the plateau and thus limited opportunity to observe Lg that did not cross the margins of the Tibetan Plateau. Though Lg is generated on the plateau, for our data set ($M_b=3.7-5.5$), we find that energy is quickly attenuated for event/station paths within the plateau that are greater than about 600-700 km. Events to the north of the Tibetan Plateau do not have observable Lg energy at recording stations within the Tibetan Plateau. This suggests that the northern

boundary of the plateau blocks L_g transmission. We do, however, observe L_g at our stations near the northern edge of the plateau for long paths (> 700 km) from the same events to the north of the plateau, suggesting that the Tarim and Qaidam Basins allow for more efficient propagation of L_g than the Tibetan Plateau. We also confirm previous observations that the southern boundary of the Tibetan Plateau blocks L_g propagation (Ruzaikin et al., 1977; Ni and Barazangi, 1983).

Figures 2a and 2b are maps showing selected paths to demonstrate the spatial distribution of L_g propagation without obscuring the important points with our abundance of data. Figure 2a shows that a majority of paths where L_g is observed are for events within the plateau. Most of these paths are short and restricted to the eastern plateau. At stations within the plateau, a small number of paths with observed L_g energy are from events outside of the plateau. In most cases the Kunlun and Himalaya ranges block L_g energy. However, in some cases from events outside of the plateau, L_g is observed at stations toward the edges of the plateau. More specifically, two stations approximately 100 km from the 4000 m contour (BUDO, GANZ) have L_g from events outside of the plateau (Figure 2a). This suggests either a transition zone of L_g attenuation or that L_g is scattered and can propagate a short distance before it is entirely "attenuated". Figure 2b shows that a majority of regional paths that cross the Tibetan plateau do not contain significant L_g arrivals. These are either long paths within or paths crossing the boundaries of the Tibetan Plateau.

Record sections are shown in Figures 3 and 4 to demonstrate L_g propagation for some paths shown in Figure 2. Event 91.222.20.21.24 is an example of an event within the Tibetan Plateau and sample seismograms are shown in Figure 3. Event 91.222.20.21.24 was, between ERDO and WNDO in the array, within the central portion of the plateau (Figure 2). For events within the plateau, recorded at stations within the plateau, L_g energy is observable out to distances of 600-700 km. Energy and frequency content steadily decrease with epicentral distance. By examining paths from many event locations, we find little correlation with L_g amplitude decay and internal plateau structure. Instead, it appears to be primarily related to path length within the plateau. Also, the previously-identified zone of inefficient S_n propagation in the northern plateau (Ni and Barazangi, 1983; McNamara et al., 1995), does not appear to have an effect on L_g amplitudes. This would suggest that the crust of the Tibetan

Plateau is laterally uniformly efficient at attenuating Lg energy while mantle properties vary across the plateau.

For paths that cross into the Tibetan Plateau there is virtually no observable Lg energy. We show an example of how the northern boundary of the plateau blocks Lg transmission using event 91.257.13.17.47 (Figure 4). This is an event from northeast of the array and shows Lg energy at stations at the northern end of the array (TUNL, MAQI, BUDO). Since the magnitude of the earthquake (91.257.13.17.47, $M_b=5.1$) is similar to events examined within the plateau, the presence of energy at TUNL and MAQI suggests that Lg will propagate at long distances (> 700 km) outside of the plateau. Lg amplitude is significantly decreased as paths propagate into the plateau. The weak presence of energy at the stations USHU and ERDO for the same event demonstrate the the boundary does not abruptly block Lg transmission. Instead energy diminishes across about 200 km of the plateau path. These observations are also significant because stations within the plateau, have similar azimuths, for these events. Therefore the absence of Lg can be attributed to the margins of the plateau rather than to the radiation patterns of the sources.

The southern boundary of the Tibetan Plateau also has a dramatic effect on Lg and has been demonstrated in previous studies (Ruzaikin et al., 1977; Ni and Barazangi, 1983). For events south of the Tibetan Plateau, the amplitude of Lg quickly dies out at stations progressively northward and into the plateau. Events 91.341.13.57.39 and 92.154.22.08.09 are located southwest of the array to the south of the Tibetan Plateau and the Himalayan boundary thrust (Figure 2). Both show practically no Lg energy at our recording stations with the exception of some southern stations (GANZ, XIGA). In these cases, Lg amplitudes are quite small and energy quickly decays progressively to the north. Ni and Barazangi (1983) suggest that the Indus-Zangbo suture zone rather than the Himalaya is the boundary that blocks Lg energy from entering the plateau. Due to our limited raypath coverage we are not able to observe this distinction.

We have shown that Lg is generated within the plateau but does not propagate efficiently to distances greater than about 600 km for our dataset ($M_b < 5.5$). This implies a high attenuation for paths within the plateau as predicted by Molnar and Oliver (1969) and Ruzaikin et al. (1977). We have also

shown that Lg energy is virtually blocked for all paths that cross the margins of the plateau defined by the Himalaya and Kunlun mountain ranges to the south and north respectively. While attenuation for Lg paths within the plateau is high, the dominant effect contributing to the demise of Lg for paths entering the plateau is at its margins. High attenuation within the plateau is, however, a significant contributing factor. In the next section, we present our inversion of observed Lg amplitudes for frequency dependent apparent Q to quantify Tibetan Plateau crustal attenuation.

Measurement of frequency dependent Lg Q within the Tibetan Plateau.

Q Inversion Method. Qualitatively, we have shown that Lg is generated within the Tibetan Plateau. We have also observed that the amplitude of Lg decreases quickly with increasing epicentral distance within the plateau. This observation implies that attenuation is high within the plateau. In order to quantify our inferred high attenuation, we have examined the amplitudes of Lg arrivals from events within the Tibetan Plateau for apparent Q (Figure 1). The quality factor, Q , is the inverse of attenuation and may provide information about the medium in which Lg propagates when compared to other regions throughout the world.

The observed amplitude of Lg on a high frequency seismogram can be modeled as:

$$A(f, D) = \frac{1}{D^\gamma} R(f) S(f) e^{-\frac{\pi f D}{v Q(f)}} \quad (2)$$

where D is the hypocentral distance, R is the receiver term which denotes site effects, S is the term which represents the individual earthquake source excitation, f is the median frequency of the data, v is the group velocity for Lg (3.5 km/sec), γ is the exponent of the geometric spreading within the medium and $Q(f)$ is the quality factor of Lg propagation within the crust. Since we do not consider the effects of scattering or radiation pattern, and assume a reasonable geometric spreading, our measure is apparent rather than intrinsic Q . Radiation effects should be minimal since Lg consists of a large number of reflected rays that distribute energy across all three components of motion. Previous seismic refraction studies demonstrate that the geometric spreading exponent is sensitive to the velocity structure of the crust (Banda et al., 1982). We follow the conventional surface wave model for Lg geometrical spreading at regional distances and use a geometrical spreading exponent of $\gamma=0.5$ (e.g. Street et al., 1975).

This has been shown to be valid for the crust in tectonically active regions such as Southern California (Frankel et al., 1990) while more stable continental interiors, such as eastern North America, are shown to have stronger geometric spreading where γ can range from 0.7 to 1.9 (Atkinson, 1989; Frankel et al., 1990). When we performed the inversion using a geometric spreading more typical for continental paths ($\gamma=1.0$), we find that values of Q for all pass-bands used were within the 95% confidence of Q values obtained with our initial assumption of $\gamma=0.5$. Finally, since Lg is not dispersive, we assume the generally accepted frequency independent group velocity of 3.5 km/sec to compute Lg travel time. We also find that the inversion is relatively insensitive to propagation velocity. Inversions using the mid-window group velocity ($v=3.4$ km/sec) did not significantly alter resultant Q values. Rewriting and taking the natural log of both sides of (2) yields:

$$\ln[A(f,D)D^\gamma] = \ln[R(f)] + \ln[S(f)] - \frac{\pi f D}{vQ(f)} \quad (3)$$

When the left-hand side of (3) is plotted against distance, (3) describes a line where the R and S terms control the intercept and the Q term controls the slope.

The technique described here is similar to the single station method proposed by Aki (1980b) where he used a set of earthquakes recorded at one station. Aki (1980b) makes use of a coda normalization in which the Lg amplitude is divided by the coda amplitude to remove the instrument response, the source excitation and the site amplification. Since the division of coda amplitude should remove the effects of site amplification, Frankel et al., (1990) extended this technique to observations of earthquakes at different stations. Since the response of our instruments is well-known (Owens et al., 1993a), we eliminate the coda normalization step and directly solve for the source and receiver terms as well as the regional $Q(f)$ by inverting instrument-corrected and geometrical spreading corrected Lg amplitudes from many different events recorded at the stations within our array (Benz et al., 1994). Using our data set of many source-receiver pairs, a system of linear equations can be set up based on equation (3) where:

$$Ax=t \quad (4)$$

A is a matrix is made up of the parameter coefficients of (3). It contains mostly ones and zeros and one column listing a portion of the last term of (3) ($-\pi f D / v$). The vector x contains the unknowns S for

each event, R for each station and the regional Q term. The t vector contains the left hand side of equation (3). By fixing f , we know A , D and v for each source-receiver pair. We then solve S for each event, R for each station, and Q using a singular value decomposition inversion technique (Menke, 1990). By performing the inversion over several frequency bands, we obtain a measure of frequency dependent $Q(f)$.

Data selection and preparation. For our analysis, we restrict our data set to events with paths confined to the Tibetan Plateau. Since we have shown that the boundaries of the plateau block Lg propagation, this step will eliminate paths with weak Lg that may contaminate the plateau measure of Q . Figure 5 is an example of the Lg phases used in the inversion. We first computed the instrument corrected, displacement seismogram of the band pass filtered tangential component of motion. Selection of the tangential component is based on the observation, from the previous section, that energy is greater and more consistent across more pass-bands on the tangential than on the vertical or radial components of motion. As a test, we ran the inversion on amplitudes measured from the vertical component and found that resulting Q values were within one standard deviation of the results acquired with tangential component amplitudes. This verifies our assumption that Lg energy is distributed across all components of motion and that fall off of amplitude with increasing distance is consistent across all components of motion. We did find, however, that at high frequencies, we were unable to obtain enough high signal-to-noise Lg phases on the vertical component to compute Q . In general, signal-to-noise was best on the tangential component for all pass-bands examined.

The filtered seismogram was then smoothed about the mean of a 10-sample moving window. Next, we determined the seismogram envelope $E(t)$ from:

$$E(t) = [A(t)^2 + H(t)^2]^{0.5} \quad (5)$$

where $A(t)$ is the smoothed, bandpassed time series and $H(t)$ is its Hilbert transform. We used the maximum amplitude within a window bounded by velocities of 3.6-3.2 km/sec for the actual inversion rather than the fall off of Lg coda (Aki, 1980b). Examples of Lg amplitudes for one event, filtered in 1 octave pass-bands are shown in Figure 5.

Prior to the inversion, Lg signal-to noise was examined to eliminate random errors in the ampli-

tude measurements. Specifically, we only wish to include amplitudes in the inversion where Lg is actually present. For the signal-to-noise analysis, shown in Figure 6, the Lg signal was taken as the average amplitude within the Lg window and the noise was measured as the average amplitude for an additional 50 seconds behind the Lg window. Figure 6 shows the signal-to-noise ratio versus epicentral distance for Lg amplitudes in the 2-4 Hz band, for paths from 52 events within the Tibetan Plateau. In many cases the signal-to-noise ratio was much greater than 10 but are not plotted so as to demonstrate the differences at low signal-to-noise ratios. For the inversion, we selected only Lg phases with a signal-to-noise ratio of 2 or greater. In Figure 6, we see that this criteria eliminates all paths within the plateau greater than about 700 km as well as all paths crossing the northern boundary of the plateau to the stations TUNL and MAQI. This observation is consistent with our qualitative amplitude observations discussed in the previous section. We also required that each station record at least two events and that each event was recorded by at least two stations. Figure 7 shows paths with Lg signal-to-noise ratios of at least 2 that were used in the inversion. This leaves 106 observations from 20 events recorded at 8 different stations. Coverage is restricted to the eastern portion of the plateau since the longer paths from western events did not contain measurable Lg energy. Therefore, our final $Q(f)$ is representative of only the eastern portion of the Tibetan Plateau due to our station coverage and small magnitudes of the events in our data set.

Results. By repeating the inversion over a range of five different fixed frequency bands we obtain a measure of frequency dependent $Q(f)$. The inversion was performed over five octaves with center frequencies of 0.75, 1.5, 3, 6 and 12 Hz. Figure 8 shows Lg amplitude data with the source and receiver contributions removed. Straight lines represent the best fitting Q for the particular frequency band. As is often observed Q increases with increasing frequency, however, our measured Q for the Tibetan Plateau is low relative to other continental regions (Benz et al., 1994). As shown in equation (1), Q can be expressed as a function of frequency. Taking the log of both of sides equation (1) yields:

$$\log [Q(f)] = \log [Q_0] + \eta \log [f] \quad (6)$$

which is an equation for a straight line where $\log [Q_0]$ is the intercept and η controls the slope. A least squares fit to the plateau data is shown in Figure 9 and gives:

$$Q(f) = (279 \pm 39.5)f^{(0.53 \pm 0.09)} \quad (0.5 \leq f \leq 16\text{Hz}).$$

Discussion

The lack of *Lg* energy for paths crossing the Tibetan Plateau has been attributed to either a change in the crustal waveguide at the boundaries of the plateau or else to complications to the waveguide within the interior of the plateau itself. The crust within the Tibetan Plateau is thicker than surrounding regions, such as the Indian Shield to the south and the Tarim Basin to the north (Molnar, 1988). *Lg* amplitude could decrease as it encounters the thickened crust of the Tibetan Plateau. Also, the complicated structures that bound the plateau, such as the southern Himalayan boundary thrust and the northern Kunlun fault, could cause scattering of *Lg* energy, significantly decreasing its observable amplitude. Causes of *Lg* attenuation due exclusively to the interior of the plateau could be attributed to an unusual velocity structure due to the anomalously thick plateau crust or else high attenuation because of scattering on crustal fractures or lateral differences in temperature within the crust (Aki, 1980a; Ruzaikin et al., 1977; Gregersen, 1984; Frankel et al., 1990). All are likely candidates to explain the observed *Lg* amplitude decrease for paths crossing the Tibetan Plateau. In the following sections we explore these ideas in more detail.

Lg attenuation at the boundaries of the Tibetan Plateau. Previous studies have reported that *Lg* is not observed for paths crossing the Tibetan Plateau (Ruzaikin et al., 1977; Ni and Barazangi, 1983). Since *Lg* is a crustal wave train, its absence can be caused by significant changes and/or anomalies in the crustal waveguide. Ruzaikin et al., (1977) have speculated that *Lg* is disrupted at the margins of the plateau by a change in crustal thickness or by the absence of the crustal "granitic layer". Alternately, they suggest that *Lg* is not efficiently propagated within the plateau at all due to extremely high intrinsic attenuation within the plateau itself. Our results suggest that both may contribute to the absence of *Lg*. We have shown that *Lg* is absent for all paths crossing the margins of the plateau. This indicates that not only the southern boundary, defined by the Himalaya, but the northern Kunlun front is equally efficient at blocking the propagation of *Lg*. Due to the lack of seismicity to the east to the plateau, in China, we were not able to examine many paths crossing the eastern boundary of the plateau. We have shown that *Lg* energy can be observed at stations near these boundaries but is quickly

decreased at stations further within the plateau. This observation suggests that the signal is scattered rather than abruptly removed. If the crustal "granitic" layer, in which Lg propagates, were completely absent within the Tibetan Plateau, then we would expect no Lg within the plateau. Since we have shown that Lg does propagate within the plateau, a variation in crustal thickness across the boundaries rather than a complete removal of the crustal waveguide, as previously suggested, is a more likely interpretation of our observations.

Lg attenuation within the Tibetan Plateau. Lg is clearly generated within the plateau; however, amplitudes are significantly diminished for paths greater than about 600-700 km for our data set. We have not observed any correlation between propagation direction or path location with the presence or absence of Lg within the plateau. This suggests that while the crustal waveguide is homogeneous enough to allow Lg to propagate, attenuation in the crust is sufficient to rapidly diminish the signal amplitude. We suggest that several geologic factors may contribute to apparent attenuation within the crust and the corresponding inefficient propagation of Lg . First is the highly fractured nature of the crust due to the numerous tectonic terranes that make up the plateau. Second is the possible lateral variation of thermal properties within the crust across the plateau. We do not yet have a good understanding of the thermal properties of the Tibetan Plateau, however, the north-central plateau has a number of seismic observations that have been interpreted as evidence for high temperatures in the upper mantle. For example previous studies, within the northern Tibetan Plateau, have reported observations of large teleseismic S - P travel time residuals (Molnar and Chen, 1984; Molnar, 1990), slow Rayleigh phase velocities (Brandon and Romanowicz, 1986), slow Pn velocities (Zhao and Xie, 1993; McNamara et al., 1994a), the absence of Sn propagation (Ni and Barazangi, 1983; McNamara et al., 1995) and large values of shear wave splitting (McNamara et al., 1994b). Each of these observations is in support of anomalous heat production beneath the northern portion of the plateau. Also, recent volcanic flows of both basaltic and granitic composition are observed at the surface throughout the northern portion of the plateau (Dewey et al., 1988). This would indicate a mantle source of volcanism causing crustal heating as it propagates toward the surface. Crustal heating is likely to significantly increase crustal attenuation (Frankel et al., 1990).

Finally, it may be possible that Lg could be disrupted by the unusually thick crust itself. The Tibetan Plateau crustal thickness is twice the continental average (Molnar, 1988). If Lg is a combination of multiply reflected crustal shear energy, a significantly thicker crustal waveguide will increase the total path length of travel for Lg energy. Any one of these or all in combination may cause a significant enough change in the crustal waveguide to contribute a weakening effect to the amplitude of Lg .

Figure 9 is a plot of Lg apparent $Q(f)$ functions obtained from a variety of sources as well as our results obtained for the Tibetan Plateau. Most results are obtained by the analysis of Lg coda rather than Lg itself. Using Figure 9 it is possible to compare our value of Lg $Q(f)$ for the Tibetan Plateau with other tectonic regions around the world as well as with previously determined values within the Tibetan Plateau. The highest values of Q_0 are for relatively stable continental paths with various frequency power law values, η (Figure 9). Low Q values are generally observed in tectonically active regions. An exception to this is the Q determined for the North Australian craton (AUS, Figure 9) (Bowman and Kennett, 1991). To explain the departure from a typical crust they argue that the geometric spreading in Australia varies from standard models.

Using a technique similar to ours Shih et al., (1994) reported a Q_0 value, for the Tibetan Plateau, considerably higher than ours with a weaker frequency dependence (TIB, Figure 9). The difference between Shih et al., (1994) and this study is likely due to differences in the respective data sets. Shih et al., (1994) examined energy in the 2.9-3.6 km/s group velocity window with a much longer period (1-6 s) than used in this study. Also, many paths used in their study crossed the margins of the plateau. Finally, the CDSN station in Lhasa (LSA) was the only station Shih et al., (1994) used within the Tibetan Plateau. Consequently event to station paths do not entirely coincide with the area covered by our study. Our study is an analysis of high frequency Lg (0.5-16 Hz) within the eastern portion of the plateau.

Direct comparison of our results to regions in North America suggest that Lg Q_0 within the Tibetan Plateau is well below the eastern and central US and slightly above the Basin and Range. This suggests that the Tibetan Plateau is more similar to a tectonically active region than a stable continental

interior or passive margin.

The crust within the Tibetan Plateau is twice as thick as the continental average and because of this, $L_g Q(f)$ comparisons, with different regions, should be made with caution. Previous authors have shown that earthquakes generally have lower $L_g Q(f)$ than explosions (Chavez and Priestley, 1986). This effect has been attributed to depth of the event itself. Ray tracing indicates that surface source explosions propagate L_g within a thin, surface waveguide, while deeper earthquakes (>10 km) propagate L_g throughout the entire crustal waveguide (Campillo et al., 1985). If waveguide thickness effects $L_g Q$ then the low $L_g Q$ of the Tibetan Plateau may be a function of the doubly thick crust (~70 km) and may not uniquely reflect the actual rock properties (i.e. intrinsic Q). For $L_g Q$ comparisons between regions of varying crustal thicknesses, values of Q may need to be corrected for waveguide thickness.

Xie and Mitchell (1991) obtained a tomographic map of the laterally varying L_g coda Q in southern Eurasia. They predict a Q_0 that increases from the south to the north from about 250 to 350 across the Tibetan Plateau. These $L_g Q_0$ values can have errors that range from about 10% to 15% (Xie, 1993). Taking into account uncertainties in the measurement procedures and assuming a close resemblance between L_g coda Q and $L_g Q$, we find that our average Q_0 of 278 ± 39.5 is in very close agreement with the median results ($Q_0 \sim 300$) obtained by Xie and Mitchell (1991) for the Tibetan Plateau. If we assume that our signal to noise criteria was successful at reducing random error from the amplitude observations, then our resultant error bars are likely a measure of the lateral heterogeneity of the attenuation structure within the Tibetan Plateau. Based on our qualitative analysis of L_g amplitudes that propagate within the plateau, we were unable to detect lateral variations. However, the roughly 14% uncertainty in our average $L_g Q_0$ indicates that such heterogeneities could exist.

The inverse method used in our analysis utilizes many source-receiver paths so consequently solves for an average regional $L_g Q$ estimate. It is likely that individual paths, or else regionalized sets of paths should be analyzed to potentially correlate variable $L_g Q$ with regional structures across the plateau. Xie (1993) has developed a method, similar to ours, in which both L_g source spectra and path dependent Q can be determined simultaneously. The technique was demonstrated to be successful using one explosion recorded at several stations in central Asia. The most significant advantage of Xie's tech-

nique is that it allows values of Q_0 and η to be variable among paths (see SIB, CAS in Figure 9). Such information would be useful to explain the uncertainties in our $Q(f)$ results however, when applied to earthquake sources, radiation pattern may be more significant than when using explosion sources. Consequently with few observations, interpretation of path-dependent Lg Q might prove difficult. Future analysis of Lg Q within the Tibetan Plateau will test the applicability of path-variable Lg Q to better explain our uncertainties with laterally heterogeneous attenuation structure within the Tibetan Plateau.

Implications for event discrimination. We can qualitatively demonstrate the significance of an accurate knowledge of regional attenuation in event discrimination efforts. Specifically, the northern boundary of the plateau effectively eliminates the ability to discriminate between naturally occurring earthquakes and nuclear explosions with the use of traditional P/Lg ratios. For example, Figure 10 shows broadband seismograms at two separate stations from an earthquake (91.257.13.17.47) and a nuclear explosion (92.142.05.00.01) at roughly equal distances to the north of our array (see Figure 2). At the station TUNL, north of the northern margin of the plateau, a clear distinction can be seen in the relative amplitudes of the P and Lg phases. Lg energy for the naturally occurring earthquake is significantly greater, relative to the first arrivals, than for the explosion. This suggests that at TUNL the P/Lg ratio would be an effective discriminate. However, for stations within the plateau (ERDO Figure 10), Lg paths from the two events cross the northern boundary of the plateau and Lg energy is not observable. In this case, P/Lg ratios are similar for these two events and a distinction cannot easily be made between the naturally occurring earthquake and the nuclear explosion using P/Lg ratios. These observations demonstrate that if restricted to analysis of event paths that cross the boundaries of the Tibetan Plateau, discrimination and yield estimation efforts, based on Lg , will be erroneous. Either additional methods or a more accurate understanding of regional variations in attenuation is required for the Tibetan Plateau.

Conclusion

Our data set represents the first observations Lg arrivals for source-receiver paths confined entirely to the Tibetan Plateau. From our qualitative analysis of Lg amplitudes we conclude that Lg is generated and does propagate within the Tibetan Plateau. However, attenuation is high and Lg is not

observed in paths greater than about 600-700 km for our data set. We find a $Lg Q$ value that is similar to values determined for the tectonically active Basin and Range of North America and significantly less than $Lg Q$ determined for typical continental interior and passive margin regions. Previous studies, that relied on distant stations, observed that Lg does not propagate through the southern boundary of the Tibetan Plateau. We have shown that for paths crossing into the plateau, all margins effectively block Lg transmission. Both the Himalayan boundary thrust to the south and Kunlun front to the north are barriers to Lg propagation due to either scattering along fractures or simply due to the change in crustal thickness across the margin.

The accurate understanding of regional variations in attenuation is critical to current efforts in seismology. The attenuation within the Tibetan Plateau and the blockage of Lg transmission at its margins have clear implications for many common nuclear monitoring discriminants such as P/Lg , and P/Sn ratios. Since any path crossing the plateau will not contain Lg and attenuation is high within the plateau for both Lg and Sn , other techniques are required for event discrimination in this region.

Acknowledgements

The authors would like to thank the many scientists and field workers who endured the hardships of the Tibetan Plateau and greatly contributed to the success of this experiment. We would especially like to thank F. Wu and R. Zeng whose persistence made this cooperative effort possible. Contributors included Chinese participants from the Institute of Geophysics, State Seismological Bureau, PRC and the Seismological Bureaus of the Qinghai Province and the Tibetan Autonomous Region. U.S. participants in the field program included F. Wu (SUNY-Binghamton), R. Busby (PIC-LDGO), R. Khuenel (Carnegie-DTM), G. Randall, G. Wagner, S. Owens and M. Salvador (USC). This project was supported by NSF grants EAR-9004428, EAR-9196115, EAR-9206815 and AFOSR contract F49620-94-1-0066DEF to USC. Q(f) inversion work was supported by LLNL in the summer of 1994, and performed under the auspices of the U.S. Department of Energy by Lawrence Livermore National Laboratory under contract W-7405-ENG-48. H. Benz wrote the original inversion computer code and supplied valuable advice on L_g propagation. G. Pavlis was instrumental in noting the importance of these observations early on. Maps were created using GMT (Wessel and Smith, 1991).

References

- Aki, K. (1980a). Scattering and attenuation of shear waves in the lithosphere, *J. Geophys. Res.*, **85**, 6496-6504.
- Aki, K. (1980b). Scattering and attenuation of shear waves in the lithosphere from 0.05 to 25 Hz, *Phys. Earth Planet. Interiors*, **21**, 50-60.
- Atkinson, G. M. (1989). Attenuation of the Lg phase and site response for the eastern Canada telemetered network, *Seismological Research Letters*, **60**, 59-69.
- Banda, E., L. W. Deichmann, L. W. Braile, and J. Ansoorge (1982). Amplitude study of the Pg phase, *J. Geophys.*, **51**, 153-164.
- Bath, M. (1954). The elastic waves of Lg and Rg along Euroasiatic paths, *Ark. Geofys.*, **2**, 295-342.
- Benz, H. M., R. Buland, and A. Frankel (1994). Source and structure studies using the U. S. national seismographic network (abstract), *Sixth annual IRIS workshop*, **7**.
- Bouchon, M. (1982). The complete synthesis of seismic crustal phases at regional distances, *J. Geophys. Res.*, **87**, 1735-1741.
- Brandon, C. and A. Romanowicz (1986). A "NO-LID" zone in the central Chang-Thang platform of Tibet: Evidence from pure path phase velocity measurements of long-period Rayleigh waves, *J. Geophys. Res.*, **91**, 6547-6564.
- Bowman, J. R. and B. L. N. Kennett (1991). Propagation of Lg waves in the North Australian craton: influence of crustal velocity gradients, *Bull. Seismol. Soc. Am.*, **81**, 592-610.
- Campillo, M., J. Plantet, and M. Bouchon (1985). Frequency-dependent attenuation in the crust beneath central France from Lg waves: data analysis and numerical modeling, *Bull. Seismol. Soc. Am.*, **75**, 1395-1411.
- Chavez, D. E. and K. F. Priestley (1986). Measurement of frequency dependent Lg attenuation in the Great Basin, *Geophys. Res. Lett.*, **13**, 551-554.
- Dewey, J. F., R. M. Shackleton, F. R. S. Chang Cheng, and S. Yiyin (1988). The tectonic evolution of the Tibetan Plateau, *Phil. Trans. R. Soc. Lond.*, **327**, 379-413.
- Ewing, W. M., W. S. Jardetzky, and F. Press (1957). *Elastic Waves in layered media*, McGraw-Hill,

- New York, NY, 380 pp.
- Frankel, A., A. McGarr, J. Bicknell, J. Mori, L. Seeber, and E. Cranswick (1990). Attenuation of high-frequency shear waves in the crust: measurements from New York state, South Africa and southern California, *J. Geophys. Res.*, **95**, 17,441-17,457.
- Gregersen, S (1984). Lg-wave propagation and crustal structure differences near Denmark and the North Sea, *Geophys. J. R. astron. Soc.*, **79**, 217-234.
- Hermann, R. B. and J. Kijko (1983). Modeling some empirical vertical component Lg relations, *Bull. Seismol. Soc. Am.*, **73**, 161-181.
- Herrin, E. and J. Richmond (1960). On the propagation of the Lg Phase, *Bull. Seismol. Soc. Am.*, **50**, 197-210.
- Kennett, B. L. N., S. Gregerson, S. Mykkeltveit, and R. Newmark (1985). Mapping of crustal heterogeneity in the North Sea via the propagation of Lg-phases, *Geophys. J. R. astron. Soc.*, **83**, 299-306.
- Knopoff, L., F. Schwab, and E. Kausel (1973). Interpretation of Lg, *Geophys. J. R. astron. Soc.*, **33**, 389-404.
- McNamara, D. E., W. R. Walter, T. J. Owens, and C. J. Ammon (1994a). Upper mantle velocity structure beneath the Tibetan Plateau determined from Pn travel time tomography, *Trans. Am. Geophys. Union*, **75**, 423.
- McNamara, D. E., T. J. Owens, P. G. Silver, and F. T. Wu (1994b). Shear wave anisotropy beneath the Tibetan Plateau, *J. Geophys. Res.*, **99**, 13,655-13,665.
- McNamara, D. E., T. J. Owens, and W. R. Walter (1995). Observations of regional phase propagation across the Tibetan Plateau, *J. Geophys. Res.*, submitted.
- Menke, W. (1990). *Geophysical data analysis: discrete inverse theory*, Academic Press, Inc., San Diego, CA.
- Mitchell, B. J. and H. J. Hwang (1987). Effect of low Q sediments and crustal Q on Lg attenuation in the United States, *Bull. Seismol. Soc. Am.*, **77**, 1197-1210.
- Molnar, P. and J. Oliver (1969). Lateral variations of attenuation in the mantle and discontinuities in the lithosphere, *J. Geophys. Res.*, **74**, 2648-2682.

- Molnar, P. and W. P. Chen (1984). S-P travel time residuals and lateral inhomogeneity in the mantle beneath Tibet and the Himalaya, *J. Geophys. Res.*, **89**, 6911-6917.
- Molnar, P. (1988). A review of geophysical constraints on the deep structure of the Tibetan Plateau, the Himalaya and the Karakoram, and their tectonic implications, *Trans. R. Soc. Lond.*, **A327**, 33-88.
- Molnar, P. (1990). S-wave residuals from earthquakes in the Tibetan region and lateral variations in the upper mantle, *Earth Planet. Sci. Lett.*, **101**, 68-77.
- Ni, J. and M. Barazangi (1983). High frequency seismic wave propagation beneath the Indian shield, Himalayan arc, Tibetan Plateau and surrounding regions: high uppermost mantle velocities and efficient propagation beneath Tibet, *Geophys. J. R. Astr. Soc.*, **72**, 665-689.
- Nuttli, O. W. (1973). Seismic wave attenuation and magnitude relations for eastern North America, *J. Geophys. Res.*, **78**, 876-885.
- Nuttli, O. W., G. A. Bollinger, and D. W. Griggs (1979). On the relation between modified mercalli intensity and body wave magnitude, *Bull. Seismol. Soc. Am.*, **69**, 893-910.
- Owens, T. J., G. E. Randall, F. T. Wu, and R. S. Zeng (1993a). PASSCAL instrument performance during the Tibetan Plateau passive seismic experiment, *Bull. Seismol. Soc. Am.*, **83**, 1959-1970.
- Owens, T. J., G. E. Randall, D. E. McNamara, and F. T. Wu (1993b). Data Report for the 1991-92 Tibetan Plateau passive-source seismic experiment, *PASSCAL Data Rep. #93-005*.
- Pec, K. (1962). Continental waves in central Europe, *Pr. Geophys. Ustern Cesk. Acad. Ved.*, **102**, 123-193.
- Press, F. and M. Ewing (1952). Two slow surface waves across North America, *Bull. Seismol. Soc. Am.*, **42**, 219-228.
- Richter, C. F. (1958). *Elementary Seismology*, W. H. Freeman, New York.
- Ruzaikin, A., I. Nersesov, V. Khalturin, and P. Molnar (1977). Propagation of *L_g* and lateral variations in crustal structure in Asia, *J. Geophys. Res.*, **82**, 307-316.
- Saha, B. P. (1961). The seismic *L_g* waves and their propagation along the granite layer of the crust of Indian sub-continent, *Indian J. Meteorol. Geophys.*, **12**, 609-618.
- Sereno, T. J. (1990). Frequency-dependent attenuation in eastern Kazakhstan and implications for

- seismic detection thresholds in the Soviet Union, *Bull. Seismol. Soc. Am.*, **80**, 2089-2105.
- Sereno, T. J., S. R. Bratt, and T. C. Bache (1988). Simultaneous inversion of regional wave spectra for attenuation and seismic moment in Scandinavia, *J. Geophys. Res.*, **93**, 2019-2035.
- Shih, X. R., K. Y. Chun, and T. Zhu (1994). Attenuation of 1-6 s Lg waves in Eurasia, *J. Geophys. Res.*, **99**, 23,859-23,874.
- Street, R. L., R. B. Herrmann, and O. W. Nuttli (1975). Spectral characteristics of the Lg wave generated by central United States earthquakes, *Geophys. J. R. astron. Soc.*, **41**, 51-63.
- Wessel, P. and W. Smith (1991). Free software helps display data, *EOS Trans. Amer. Geophys. U.*, **72**, 445-446.
- Xie, J. and B. J. Mitchell (1991). Lg coda Q across Eurasia, *Yield and Discrimination Studies in Stable Continental Regions*, 77-91.
- Xie, J (1993). Simultaneous inversion for source spectrum and path Q using Lg with application to three Semipalatinsk explosions, *Bull. Seismol. Soc. Am.*, **83**, 1547-1562.
- Zhao, Lian-She and J. Xie (1993). Lateral variations in compressional velocities beneath the Tibetan Plateau from Pn traveltime tomography, *Geophys. J. Int.*, **115**, 1070-1084.

Figure Captions

Figure 1. Tibetan Plateau experiment base map showing recording stations (grey diamonds) and the distribution of regional events (solid circles) used to map Lg propagation. Regional structural trends are taken from Dewey et al. (1988). Solid lines show major faults and dashed lines indicate suture zones that bound tectonic terranes of the plateau. Elevation is shown shaded with 1000 m contour intervals. The area in white is above 4000 m elevation.

Figure 2. Lg propagation characteristics across the plateau. Events selected to demonstrate Lg characteristics are shown with an open circle. Event identifiers are the same as in Table 2. (a) Map of paths where Lg is not observed. (b) Map of paths where Lg is observed.

Figure 3. Central plateau event record section (91.222.20.21.24, $M_b=5.4$). Both the tangential (left) and radial (right) components of motion are shown high pass filtered (> 0.5 Hz) with the exception of LHSA. Data at the LHSA station was obtained at a slower sampling rate of 5 samples/s. Consequently, seismograms are shown band pass filtered with corner frequencies of 0.5 and 2.0 Hz. Dashed lines show the predicted arrival times of P_n (8.1 km/s), S_n (4.6 km/s) and Lg (3.5 km/s) (McNamara et al., 1995). The recording station is shown at the end of each record section trace.

Figure 4. Regional event, from northeast of the plateau, (91.257.13.15.47, $M_b=5.1$). Display parameters are the same as Figure 3.

Figure 5. An example of Lg amplitudes measured in 5 passbands used in the inversion. Event 92.143.05.46.46 ($M_b=4.6$) from the southeastern Tibetan Plateau, recorded at USHU, at a distance of 356 km. Traces are scaled individually to show the relative amplitudes of the P and Lg phases. (a) Instrument corrected displacement seismograms. (b) Envelopes of displacement seismograms in (a). (a) Tangential component of the instrument corrected displacement seismograms for passbands used in the inversion. (b) Envelopes of seismograms in (a). Lg amplitude was taken as the maximum amplitude within the window between 3.6-3.2 km/sec.

Figure 6. L_g signal to noise versus epicentral distance in the 2-4 Hz band, for 52 events located within the Tibetan Plateau. Closed squares show the average amplitude between 3.6-3.2 km/sec divided by the average amplitude for 50 sec beyond the L_g window for paths confined to the Tibetan Plateau. Open squares show signal to noise for paths that cross the northern boundary of the plateau to TUNL and MAQI. Paths with signal to noise of 2 or greater were used in the inversion for Q .

Figure 7. Paths with L_g signal to noise equal to or greater than 2.

Figure 8. Best fit Q determined from the inversion over several pass-bands.

Figure 9. The least-squares fit to our data (TP) for $Q(f)$. Also shown are several other regions for comparison including the northeastern United States (NEUS), central United States (CUS), Basin and Range province of North America (BRP) (Benz et al., 1994), Russian explosion recorded in central Asia (CAS) and stations in Siberia (SIB) (Xie, 1993), eastern Canada (ECAN) (Atkinson, 1989), eastern Kazakstan (EKAZ) (Sereno, 1990), Scandinavia (SCAN) (Sereno et al., 1988), Australia (AUS) (Bowman and Kennett, 1991), and a previously determined value for the Tibetan Plateau (TIB) (Shih et al., 1994). Axes are displayed as both frequency versus apparent Q and log frequency versus log apparent Q .

Figure 10. Broadband vertical component seismograms demonstrate the ineffectiveness of P/L_g ratios in event discrimination within the Tibetan Plateau. Seismograms are shown for two stations. One outside of the plateau, TUNL, and one within the plateau, ERDO, illustrating L_g blockage. Note the much larger P/L_g value for the explosion than for the earthquake at TUNL. At ERDO the P/L_g ratios are comparable. The L_g group velocity (3.6-3.2 km/s) is shown within the box. Note the azimuths from the earthquake to stations TUNL and ERDO differ by only a few degrees suggesting that the effect is not due to radiation pattern of the source. Epicentral distances are shown next to each trace. (a) Earthquake from northeast of the plateau (91.257.13.15.47, $M_b=5.1$). (b) Underground nuclear explosion from north of the Tibetan Plateau at the Chinese Lop Nor test site (92.142.05.00.01, $M_b=6.5$). Explosion P waves at TUNL are clipped.

Table 1

Tibetan Plateau Seismic Experiment
(Station Locations)

Station	Latitude (°N)	Longitude (°E)	Elevation (meters)
AMDO	32.247	91.688	4712
BUDO	35.529	93.910	4660
ERDO	34.520	92.707	4623
GANZ	29.767	94.050	3150
LHSA	29.702	91.128	3700
SANG	31.024	91.700	4740
TUNL	36.199	94.815	3133
WNDO	33.448	91.904	4865
XIGA	29.234	88.851	3865
MAQI	34.478	100.249	3823
USHU	33.011	97.015	3727

Table 2. Regional Events used in Lg Analysis

Event ID†	Origin Time YRDAYHHMMSS.t	Latitude (°N)	Longitude (°E)	Depth (Km)	Mb	#stations
91.193.21.55.49	91193220600.2	39.421	94.832	16	4.8	4
91.199.09.53.55	91199095036.7	8.224	94.112	27	5.4	5
91.199.13.23.31	91199132459.9	30.363	94.870	33	5.0	9
91.199.15.27.32	91199152405.1	8.439	94.629	16	5.1	1
91.199.17.44.50	91199174543.5	30.362	94.667	33	4.2	6
91.201.18.52.00	91201185223.9	30.298	94.741	33	4.5	7
91.201.18.52.05	91201190230.6	30.326	94.838	24	4.8	9
91.204.13.29.37	91204132547.3	3.775	95.932	47	5.8	8
91.204.16.50.24	91204165154.0	30.269	94.820	33	4.7	9
91.205.06.06.43	91205060644.5	30.302	94.785	33	4.8	7
91.206.01.52.18	91206015245.2	30.317	94.791	33	4.8	7
91.209.23.57.54	91209235820.2	30.329	94.793	33	4.9	8
91.210.03.18.45	91210032015.6	30.294	94.765	33	4.6	5
91.210.15.47.13	91210154808.8	30.269	94.793	33	4.7	9
91.211.22.21.39	91211222205.9	30.385	94.795	33	4.8	8
91.215.08.38.02	91215083317.1	29.330	129.081	17	5.5	2
91.216.12.42.55	91216123824.5	23.888	95.859	43	4.7	8
91.218.02.21.24	91218021731.6	3.827	95.374	18	6.0	6
91.220.11.15.33	91220111238.4	26.879	65.848	53	5.3	10
91.222.20.21.24	91222202151.7	33.910	92.158	10	4.7	11
91.231.06.07.09	91231060551.3	46.944	85.302	30	5.5	8
91.234.03.53.11	91234035341.1	25.030	91.330	33	4.7	9
91.234.21.26.07	91234211504.5	55.771	114.364	23	5.2	1
91.235.07.39.13	91235073625.8	36.155	68.802	33	4.9	5
91.236.17.46.43	91236174523.3	38.441	75.213	33	4.7	4
91.237.05.04.30	91237050059.8	5.649	94.116	44	5.2	7
91.238.20.45.55	91238204231.8	6.937	94.531	26	5.4	9
91.238.20.54.25	91238205423.0	6.882	94.609	22	5.8	8
91.239.05.14.10	91239051432.3	34.249	92.161	33	3.4	9
91.242.14.30.58	91242143212.8	34.449	97.309	33	4.3	8
91.245.11.05.48	91245110550.4	37.440	95.402	10	5.5	11
91.247.08.35.12	91247083233.5	10.746	92.843	33	5.1	8
91.247.22.31.26	91247222721.7	15.204	120.404	21	5.6	3
91.250.03.00.10	91250030024.3	24.252	93.976	33	4.9	7
91.251.23.53.44	91251235441.5	36.626	98.553	23	4.8	8
91.252.21.54.32	91252215450.5	28.879	94.937	33	4.8	11
91.255.00.45.09	91255003330.7	54.905	111.112	25	5.1	3
91.255.23.05.10	91255230630.1	29.698	95.688	34	4.6	7
91.257.13.17.47	91257131639.7	40.171	105.046	25	5.1	10
91.258.00.23.59	91258002050.3	30.617	66.735	33	4.8	5
91.258.02.15.33	91258021224.9	30.724	66.763	26	4.6	5
91.260.18.53.51	91260185322.2	43.141	87.968	22	4.8	4
91.262.04.23.29	91262042356.7	26.323	92.211	33	4.7	6
91.263.09.41.20	91263093742.5	44.832	90.332	33	4.8	2
91.263.11.15.36	91263111611.5	36.191	100.063	13	5.5	10
91.265.05.45.35	91265054227.8	30.165	67.799	10	4.9	1
91.270.07.39.55	91270073955.3	34.645	98.874	33	4.7	7
91.270.11.55.24	91270115640.8	29.911	90.423	33	3.7	5
91.270.23.29.56	91270233121.4	32.444	93.354	33	4.3	8
91.273.09.47.58	91273094442.1	22.535	121.479	24	5.5	7
91.273.16.33.41	91273163306.2	37.766	101.323	20	5.3	11

91.273.18.35.45	91273183544.2	22.728	94.416	75	4.7	10
91.274.20.33.26	91274203020.0	35.705	65.512	12	5.3	10
91.279.10.58.20	91279105044.4	21.384	104.231	10	4.5	3
91.279.12.16.45	91279121812.0	37.677	101.437	10	4.1	3
91.285.05.12.00	91285050836.3	22.798	121.536	8	5.1	3
91.285.12.23.03	91285122347.2	37.791	101.176	36	4.3	5
91.288.19.11.31	91288191100.9	30.565	79.311	33	4.5	2
91.292.21.24.47	91292212314.3	30.780	78.774	10	6.5	11
91.293.05.34.33	91293053226.8	30.790	78.686	27	4.9	2
91.296.20.41.02	91296203709.1	20.836	122.158	29	4.4	2
91.298.14.44.00	91298144039.8	23.788	122.952	27	5.2	3
91.304.02.31.18	91304022902.5	40.148	72.841	21	5.2	10
91.307.00.03.04	91307000225.9	28.365	103.984	33	4.5	2
91.312.15.16.59	91312151344.1	26.323	70.607	22	5.6	11
91.319.19.56.36	91319195343.5	29.696	69.134	19	4.6	6
91.320.12.17.40	91320121422.5	37.660	66.469	33	4.8	3
91.323.01.03.09	91323010418.0	32.484	93.593	33	4.9	10
91.325.13.36.25	91325133742.1	33.714	90.337	33	4.3	9
91.328.07.34.25	91328073526.6	33.980	88.646	33	4.7	8
91.329.10.07.40	91329100839.0	34.017	88.832	33	4.4	9
91.330.15.30.17	91330153114.7	33.919	88.746	33	4.1	8
91.330.21.15.51	91330211559.9	34.073	94.247	33	4.3	10
91.336.19.44.36	91336194536.6	32.090	94.694	46	4.4	9
91.337.13.19.49	91337131644.1	9.095	92.470	37	4.7	4
91.338.03.27.07	91338032724.2	24.015	93.986	72	4.9	11
91.339.15.51.42	91339154820.7	22.544	121.450	17	4.6	3
91.341.13.57.39	91341135740.6	24.059	93.913	69	5.1	11
91.341.14.26.09	91341142232.2	25.191	62.974	30	5.2	4
91.343.01.03.52	91343010246.5	29.543	81.632	29	5.6	11
91.348.08.19.24	91348082023.8	33.976	88.840	33	5.1	8
91.349.15.58.26	91349155932.8	29.970	93.928	33	4.8	9
91.351.20.26.50	91351202749.6	33.990	88.904	33	4.6	9
91.351.23.51.10	91351234954.5	44.333	83.727	17	4.9	5
91.353.18.59.32	91353185517.4	28.102	57.304	27	5.3	3
91.354.02.05.53	91354020605.3	24.720	93.103	41	5.3	10
91.355.19.52.42	91355195245.5	27.904	88.139	57	4.9	9
91.357.01.57.23	91357015825.1	33.917	88.863	33	5.2	8
91.357.02.14.54	91357021454.5	33.966	88.942	33	5.0	9
91.358.21.26.32	91358212752.1	30.003	92.544	33	4.4	6
91.359.12.16.26	91359121322.3	10.607	93.906	40	4.7	6
91.360.13.26.42	91360132417.7	30.837	99.532	33	4.1	5
91.361.09.11.27	91361090937.5	51.019	98.150	14	5.8	10
91.362.09.14.39	91362090703.3	51.096	98.061	17	5.0	5
91.365.21.13.33	91365211418.5	30.657	99.571	33	4.5	8
92.002.02.34.36	92002023537.2	33.990	88.859	33	4.8	9
92.004.03.37.35	92004033521.6	31.954	69.991	29	5.0	9
92.005.17.23.27	92005171421.0	40.873	71.172	16	5.0	2
92.005.17.30.00	92005172319.8	41.583	71.556	33	4.4	2
92.007.16.23.40	92007162309.9	30.118	99.537	36	4.8	8
92.008.17.40.21	92008174141.5	30.137	92.449	33	4.0	5
92.011.06.19.51	92011061655.9	9.311	86.964	22	5.7	8
92.012.00.11.55	92012001227.1	39.671	98.300	22	5.4	6
92.013.18.36.22	92013183632.1	24.439	92.557	33	4.5	5
92.020.09.01.16	92020085822.5	27.398	65.994	27	5.2	7

92.021.22.10.43	92021220758.9	26.632	67.198	26	5.4	8
92.022.21.43.49	92022214125.9	35.351	121.109	33	5.1	6
92.023.10.25.28	92023102626.7	34.566	93.164	33	5.2	5
92.024.05.06.18	92024050447.3	35.515	74.529	47	5.4	6
92.025.15.16.29	92025151231.9	26.070	98.668	33	4.7	1
92.030.05.25.29	92030052201.4	24.958	63.141	29	5.5	3
92.034.15.43.19	92034154422.6	34.496	93.147	10	4.7	6
92.036.11.04.57	92036105713.0	50.260	100.168	45	4.4	1
92.036.19.42.54	92036193629.8	31.513	67.038	33	4.4	1
92.036.23.13.35	92036231048.6	31.426	66.825	18	5.1	6
92.036.23.43.40	92036234136.8	31.365	66.858	33	5.0	4
92.037.03.34.31	92037033515.3	29.610	95.521	15	5.6	6
92.040.12.44.12	92040124452.7	29.627	95.646	10	5.1	6
92.040.14.36.56	92040143734.7	29.660	95.607	10	4.8	2
92.041.12.42.34	92041123857.1	21.173	121.901	22	5.0	2
92.045.08.21.20	92045081825.7	53.897	108.866	21	5.3	3
92.054.20.07.30	92054200625.2	41.556	81.267	33	4.7	1
92.065.02.15.19	92065021417.6	35.625	80.585	36	4.7	3
92.067.06.31.49	92067062855.3	40.075	71.685	25	4.9	3
92.067.22.40.50	92067224150.8	29.442	89.370	113	4.3	5
92.069.17.02.51	92069165928.6	27.424	66.044	19	4.9	7
92.075.01.05.37	92075010127.1	23.548	123.562	31	5.7	8
92.076.01.18.29	92076011855.9	34.343	86.288	33	4.7	6
92.077.02.17.41	92077021449.6	9.216	92.833	67	4.8	8
92.079.06.38.32	92079063425.8	17.155	120.827	15	5.7	4
92.082.01.51.00	92082014755.0	10.553	93.904	33	4.9	5
92.084.19.32.48	92084193210.3	31.545	81.540	16	4.8	3
92.084.21.04.01	92084210147.5	33.832	72.905	14	5.0	9
92.085.17.19.11	92085171537.6	24.455	123.318	78	5.4	3
92.087.10.41.40	92087103930.6	35.997	72.548	35	4.9	7
92.088.10.20.59	92088101741.8	26.582	67.303	10	4.9	6
92.090.18.27.39	92090183006.6	31.929	94.465	33	3.9	9
92.090.19.22.19	92090191934.8	35.855	72.374	55	4.4	1
92.092.13.40.48	92092134103.9	27.392	87.065	33	4.3	4
92.092.20.54.29	92092205403.7	31.964	83.754	52	4.1	3
92.095.17.42.50	92095174320.7	28.147	87.979	33	4.9	9
92.096.07.47.27	92096074747.6	35.696	80.661	18	5.5	9
92.096.11.08.11	92096110923.1	35.665	80.599	33	4.0	2
92.097.19.49.55	92097194911.3	44.427	101.792	33	4.7	2
92.103.18.41.18	92103183716.5	29.515	131.396	39	5.6	1
92.104.03.46.58	92104034751.0	31.958	88.339	33	4.6	9
92.109.18.19.52	92109181929.2	36.155	92.538	10	4.1	9
92.110.18.35.29	92110183219.0	23.861	121.594	16	5.8	1
92.111.18.49.38	92111185028.3	27.256	92.077	33	4.6	7
92.114.12.25.22	92114122117.2	29.429	131.364	40	5.8	1
92.114.14.19.00	92114141835.1	22.437	98.904	12	5.8	10
92.114.15.33.13	92114153249.1	22.418	98.852	10	5.9	10
92.114.17.20.05	92114171502.7	22.309	98.856	33	4.7	8
92.114.18.24.18	92114181811.6	22.303	98.997	33	4.8	7
92.115.07.10.45	92115070723.9	27.550	66.065	25	5.9	9
92.115.12.04.17	92115114912.3	23.768	121.660	18	4.7	2
92.119.01.36.25	92119013628.9	32.145	85.066	33	3.8	4
92.119.21.08.48	92119210303.6	22.430	98.935	33	4.6	3
92.122.08.10.36	92122080945.0	19.583	94.419	55	4.6	4

92.125.10.57.33	92125105422.2	29.882	67.550	10	4.9	5
92.130.07.23.48	92130072344.8	34.503	84.774	10	4.6	3
92.131.04.06.36	92131040432.9	37.207	72.913	33	5.6	9
92.132.11.21.35	92132112341.4	36.794	73.487	33	4.7	2
92.136.08.10.26	92136080802.9	41.019	72.429	50	5.7	6
92.137.08.34.31	92137083257.7	23.262	99.939	33	4.6	2
92.137.20.20.20	92137201952.9	36.080	99.869	17	5.0	8
92.139.19.55.16	92139195538.8	34.858	86.331	33	4.1	6
92.141.12.22.51	92141122032.8	33.377	71.317	16	6.0	9
92.142.05.00.01	92142045957.5	41.604	88.813	00	6.5	8
92.143.05.46.46	92143054731.5	30.748	99.685	33	4.6	6
92.146.05.10.38	92146050813.1	36.701	71.046	48	4.9	6
92.147.19.00.39	92147185654.8	20.100	121.396	53	4.9	1
92.154.22.08.09	92154220745.3	28.984	81.913	56	5.2	9
92.155.01.59.24	92155015513.3	28.083	128.094	56	4.9	1
92.155.02.41.37	92155024236.6	33.905	88.893	10	4.6	7
92.157.00.26.01	92157002343.7	33.241	71.228	33	4.9	6
92.162.13.41.31	92162134124.9	25.660	96.758	33	4.7	5
92.165.16.56.33	92165165507.7	39.845	77.828	35	4.7	3
92.167.02.49.28	92167024856.2	24.027	95.932	17	5.8	5
92.173.08.07.07	92173080746.5	30.428	89.394	28	4.2	2
92.173.11.11.02	92173111939.7	38.307	99.423	20	4.8	3
92.179.02.14.16	92179021318.3	35.148	81.079	33	4.5	4
92.179.13.22.17	92179132120.9	35.139	81.131	33	5.0	4

† based on the notation of Owens et al (1993b).

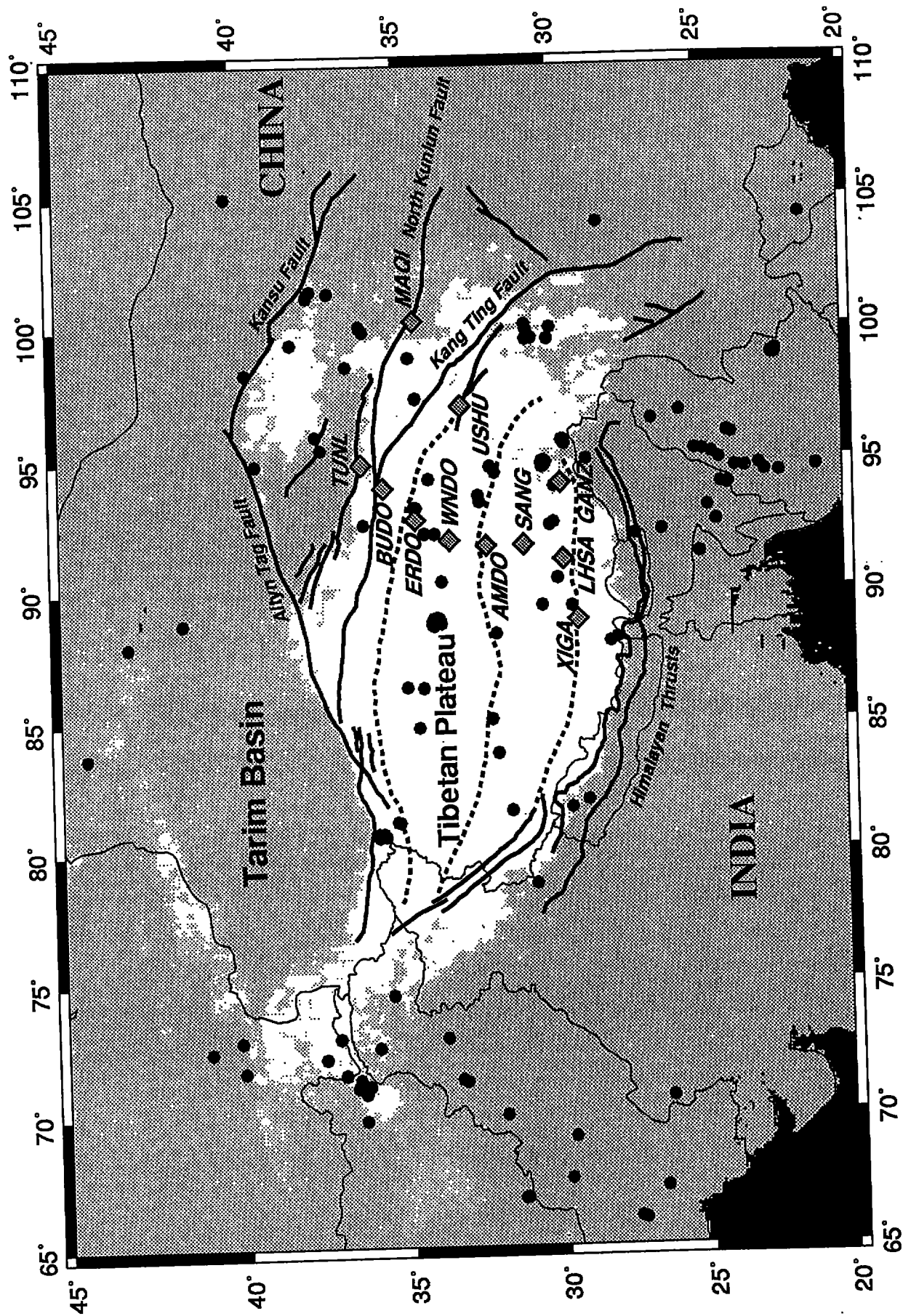
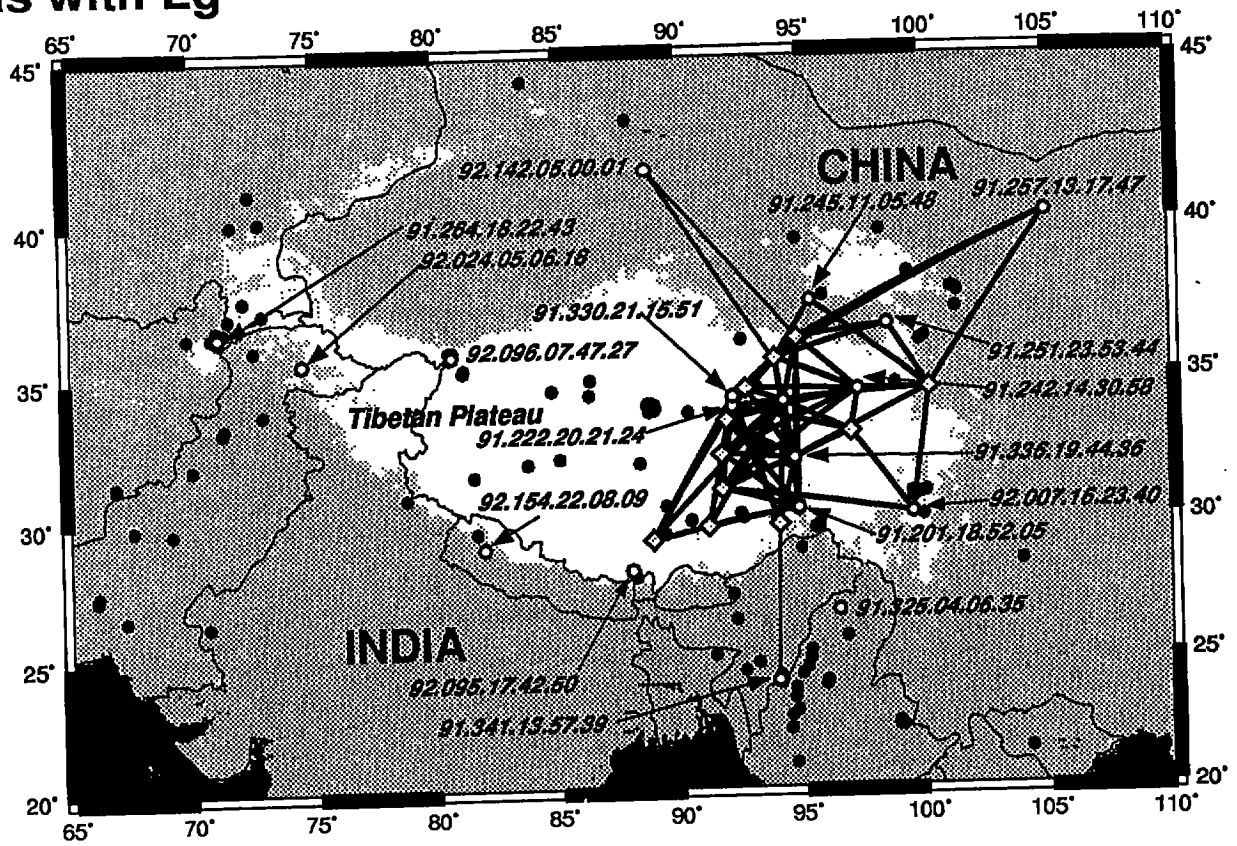


(Figure 1: McNamara et al., 1995)

A: Paths with Lg



B: Paths without Lg

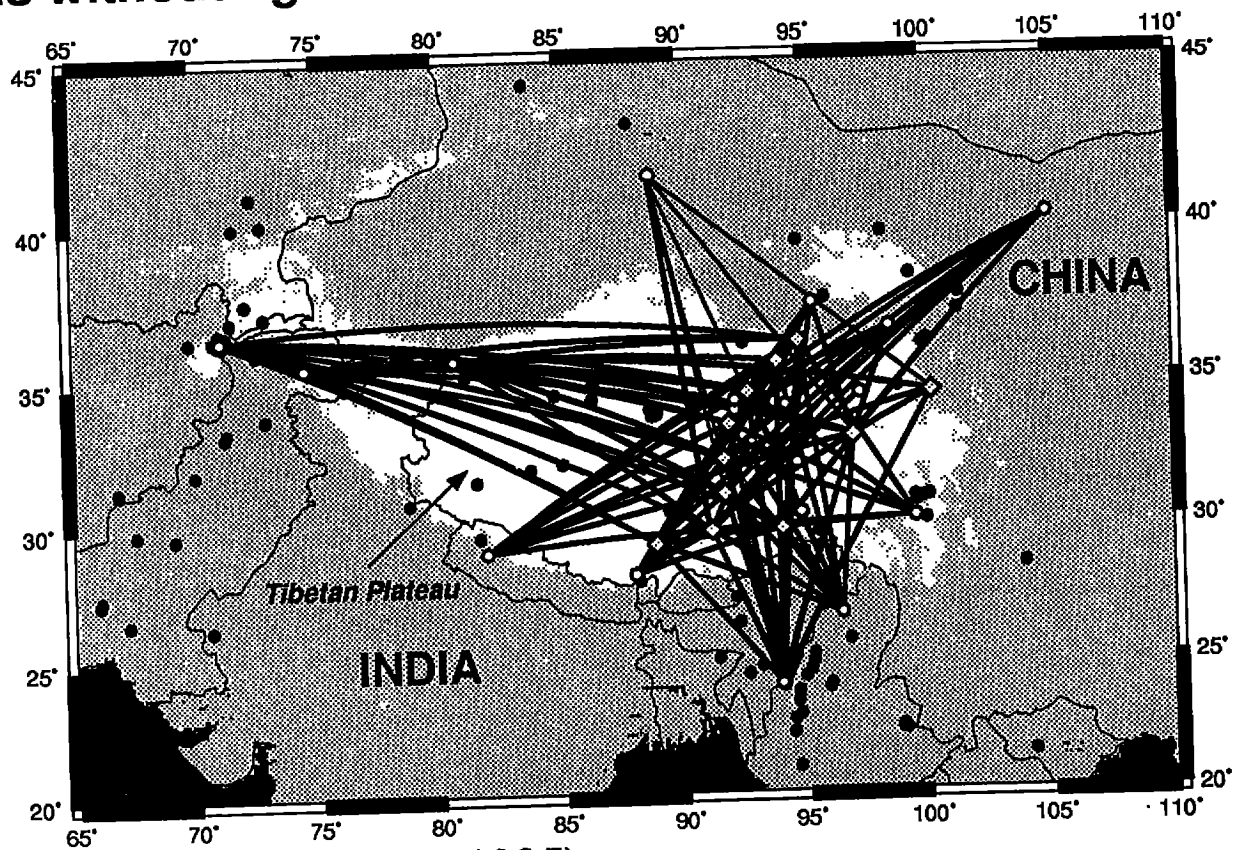
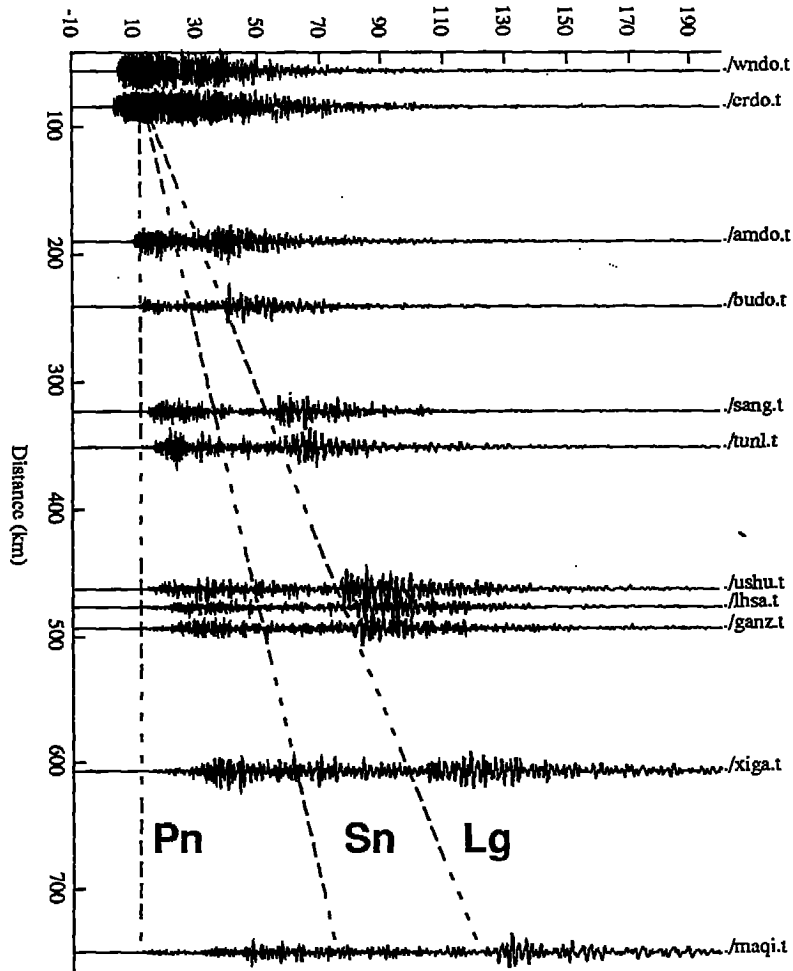


(Figure 2: McNamara et al., 1995)

(Figure 3: McNamara et al., 1995)

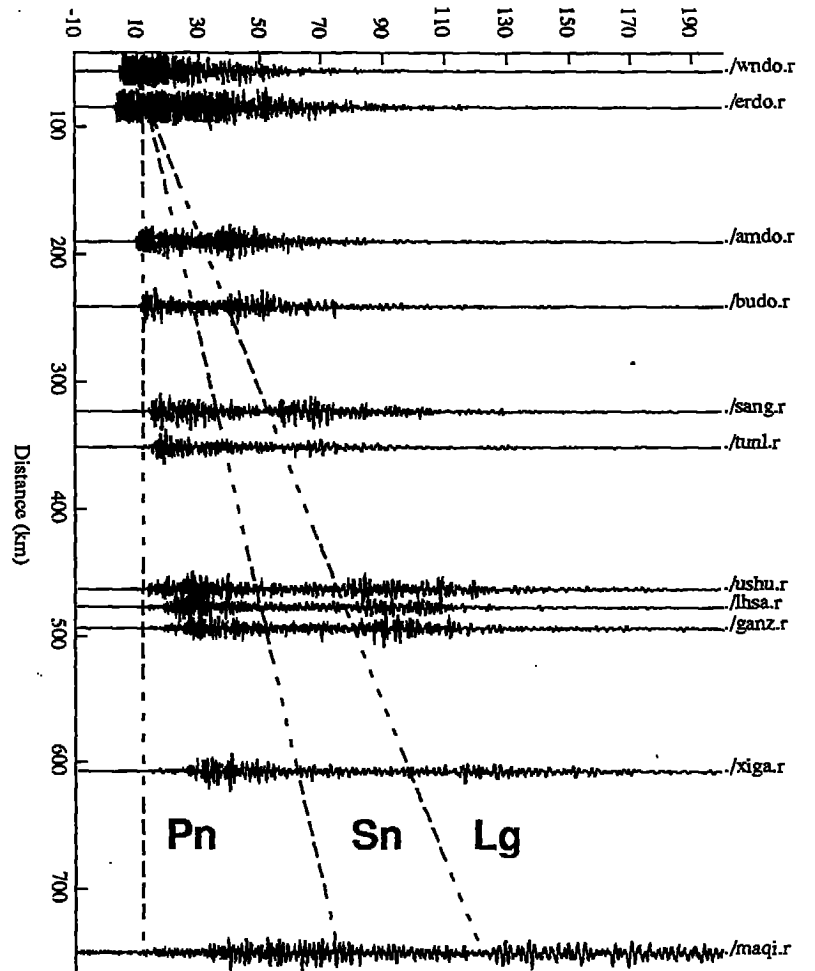
91.222.20.21.24 Tangential

Reduced Time (sec), $V_r = 8.100$ km/s

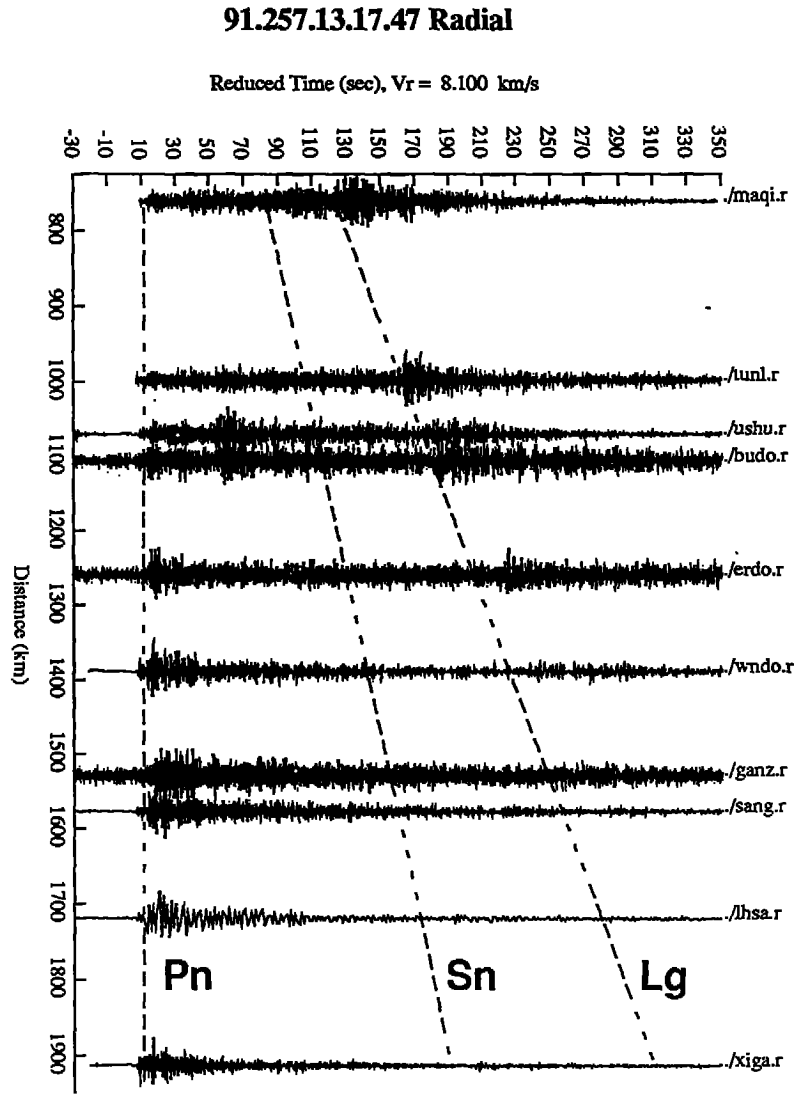
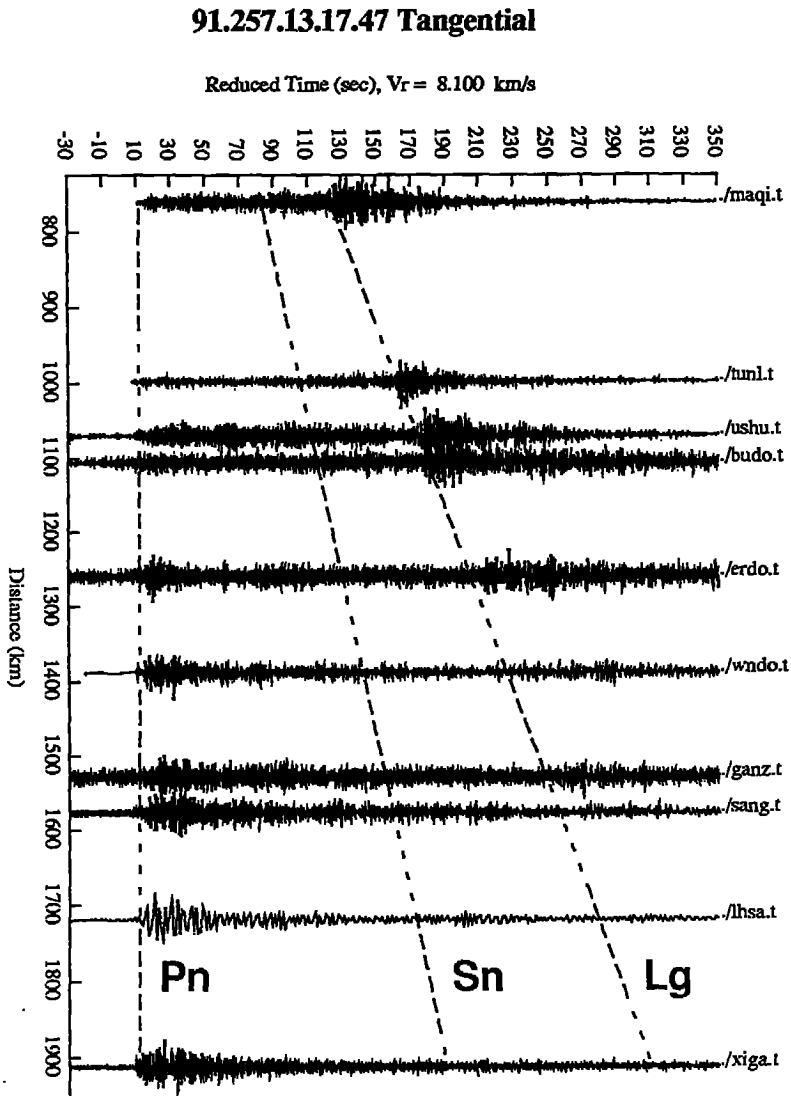


91.222.20.21.24 Radial

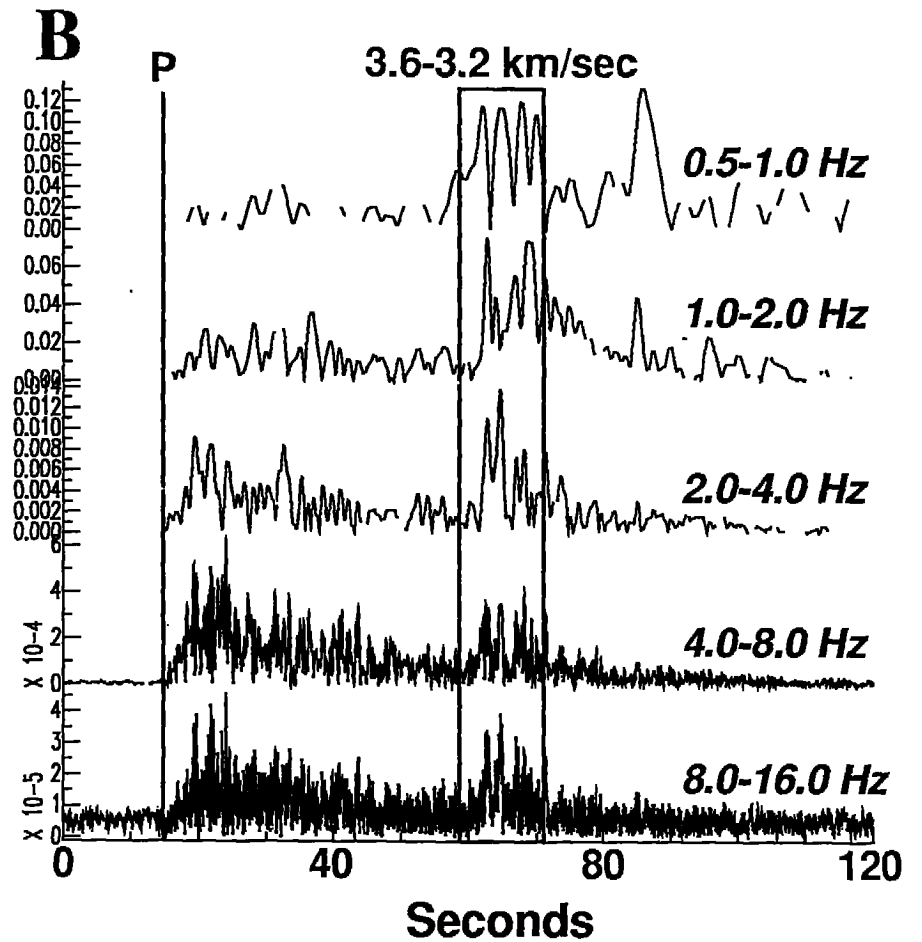
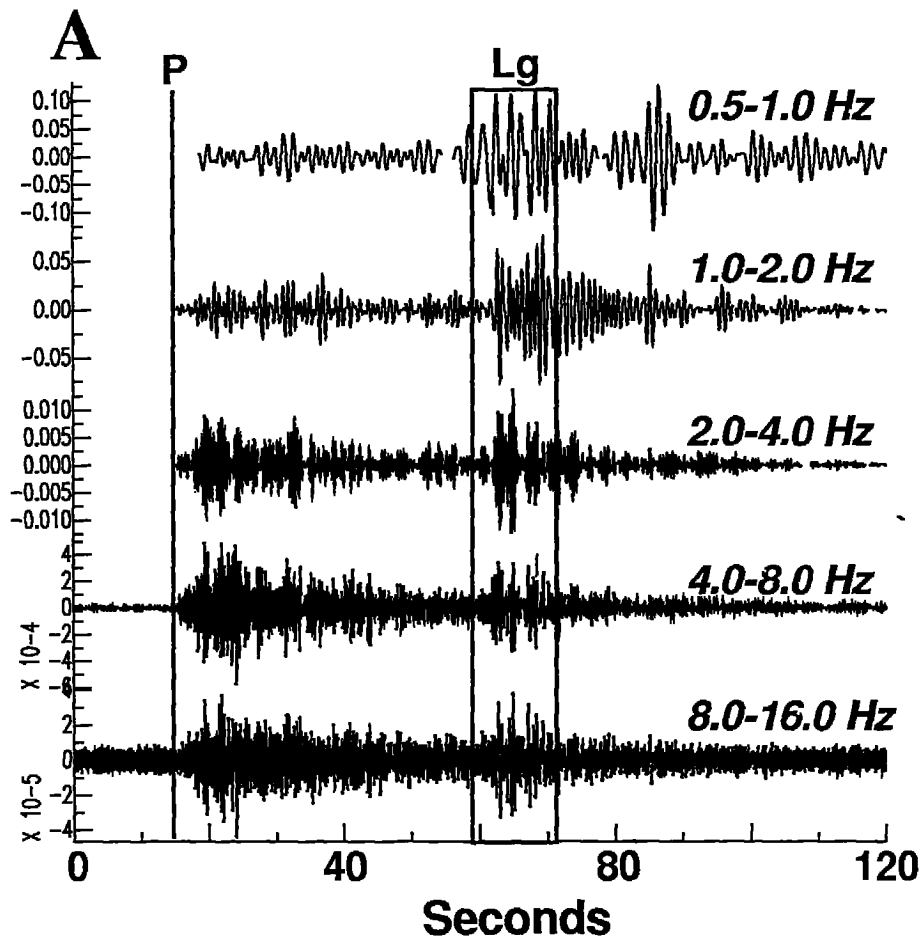
Reduced Time (sec), $V_r = 8.100$ km/s

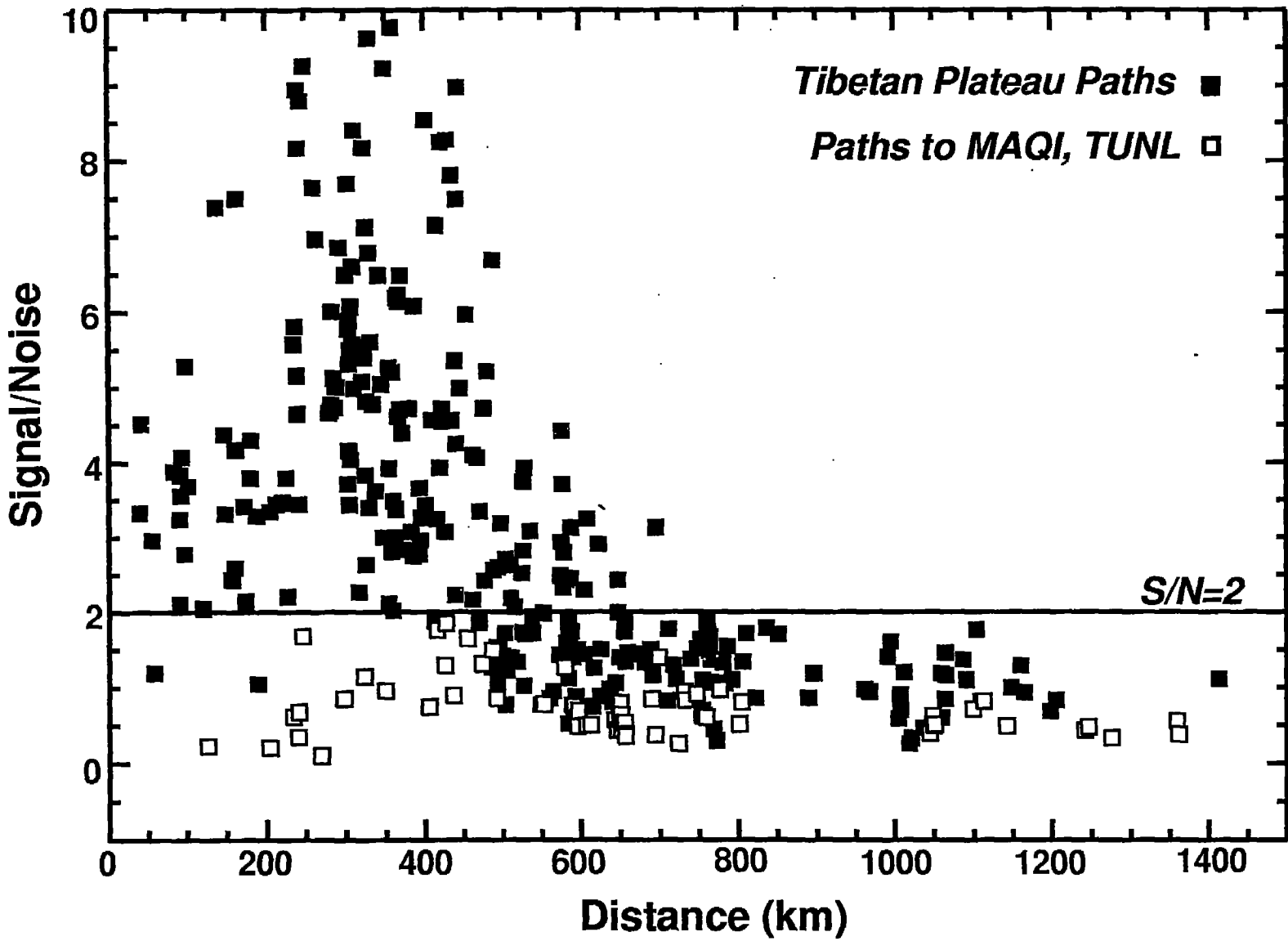


(Figure 4: McNamara et al., 1995)



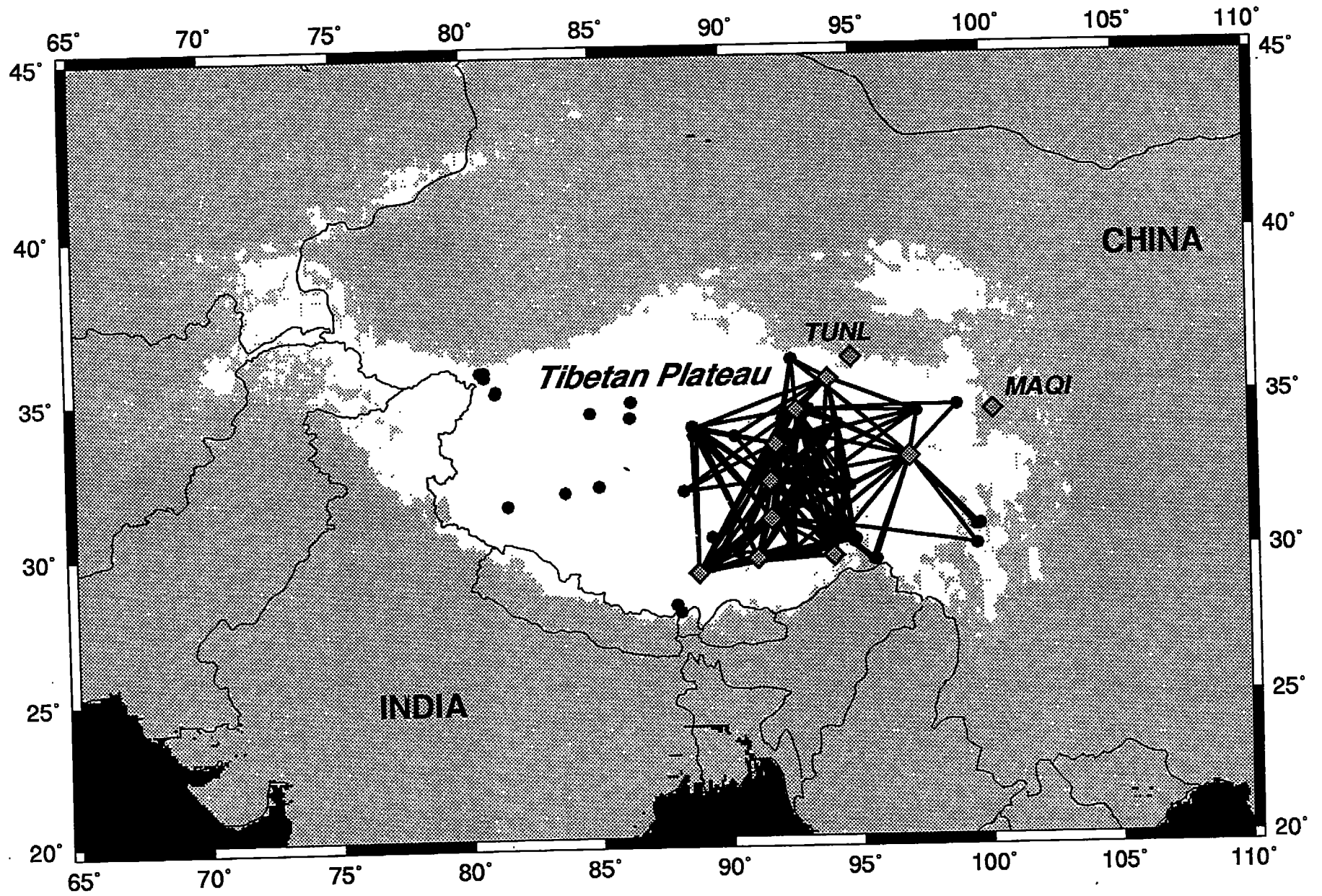
(Figure 5: McNamara et al., 1995)





(Figure 6: McNamara et al., 1995)

(Figure 7: McNamara et al., 1995)



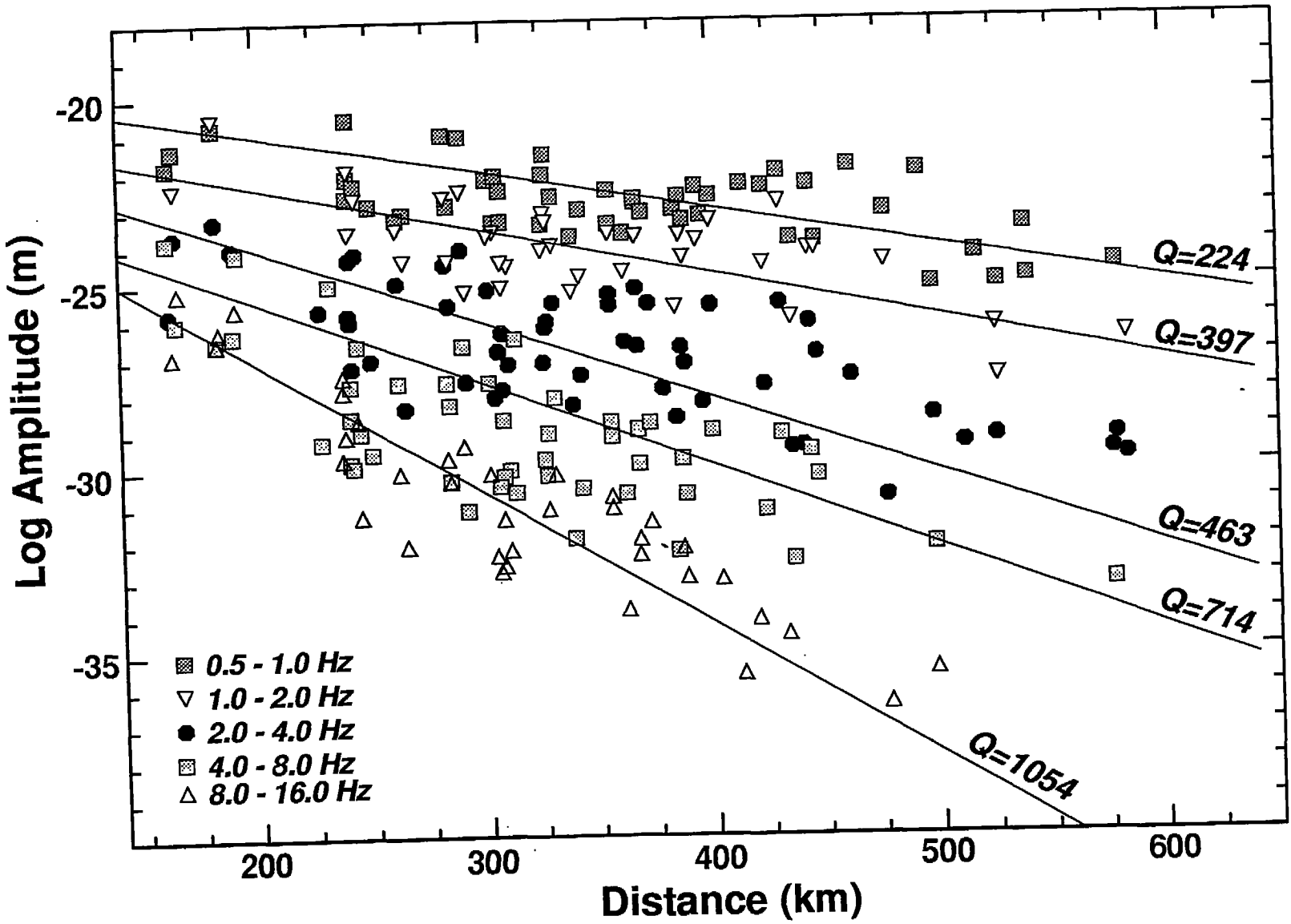


(Figure 8: McNamara et al., 1995)

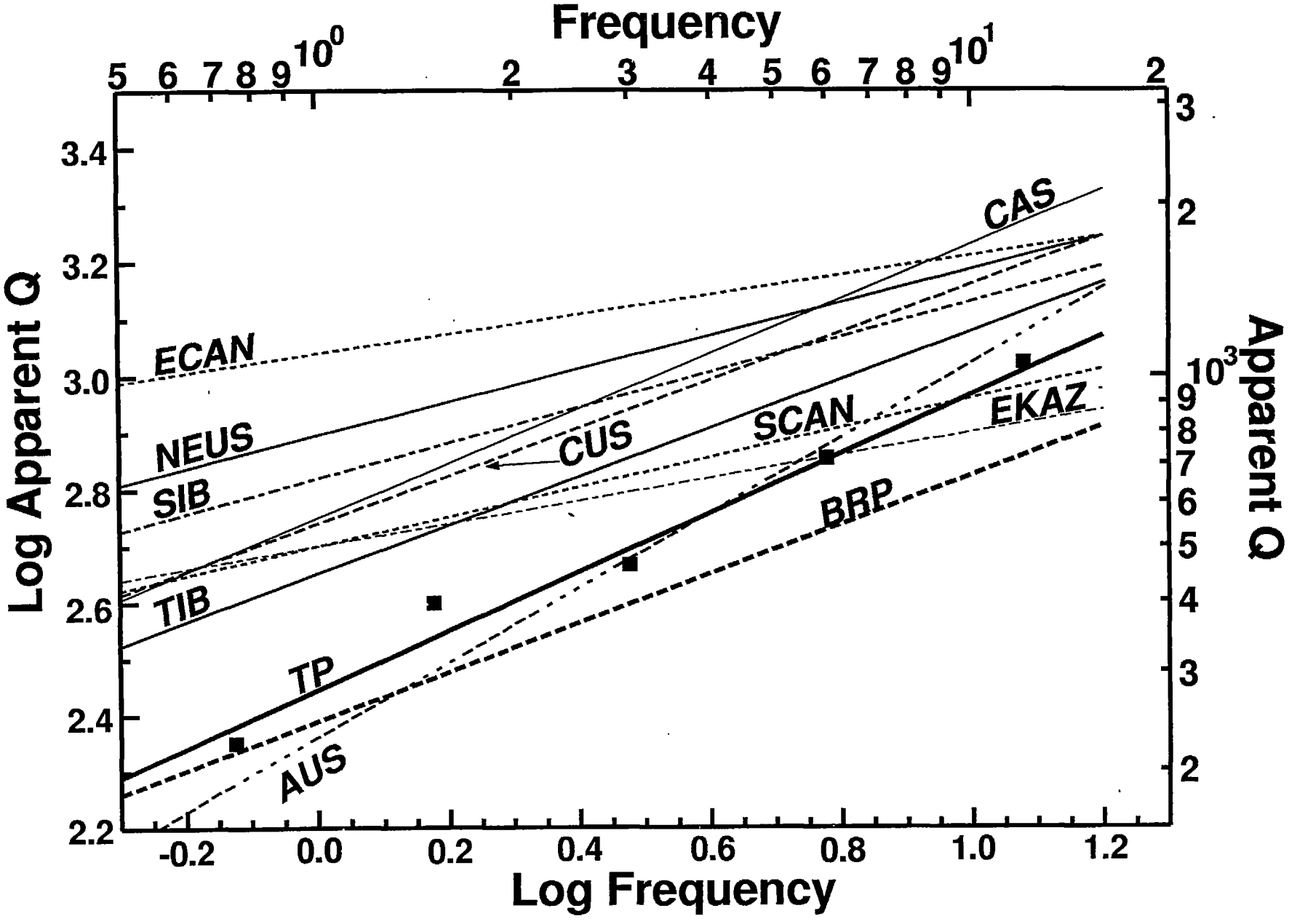


(Figure 9: McNamara et al., 1995)

Lg Blockage can affect P/Lg based discriminants

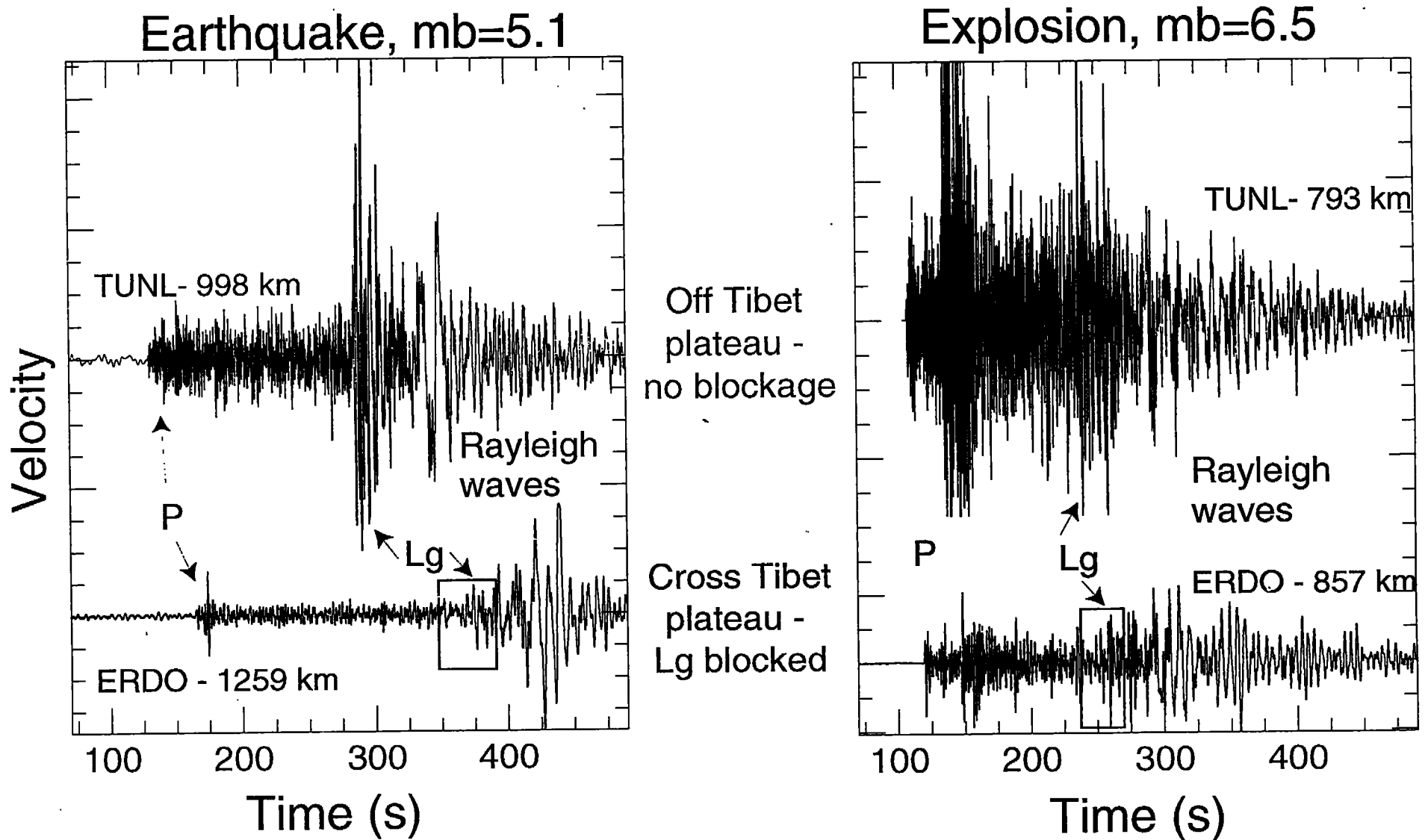


(Figure 10: McNamara et al., 1995)